ESC European Society of Cardiology

Europace (2025) **27**, euaf134
https://doi.org/10.1093/europace/euaf134

EHRA DOCUMENT

EHRA European Heart Rhythm Association

Regionalization of the atria for 3D electroanatomical mapping, cardiac imaging, and computational modelling: a clinical consensus statement of the European Heart Rhythm Association and the European Association of Cardiovascular Imaging of the ESC

Till F. Althoff (Chair) [1,2]*, Robert H. Anderson [3], Christian Goetz [4,5], Steffen E. Petersen [6,7], Patricia Martínez Díaz [5], Robin Nijveldt [8], Pal Maurovich-Horvat [9], Jeroen Bax [10], Sachal Hussain [11], Constanze Schmidt [4], Diane E. Spicer [12], Damian Sanchez-Quintana [13], Cristiana Corsi [11], Olaf Dössel [5], Andreu M. Climent [14], Blanca Rodriguez[15], Ulrich Schotten [16], Axel Loewe [5], Maria S. Guillem[14], José-Ángel Cabrera [17], and Jose L. Merino [18]

Document Reviewers: Adrianus P. Wijnmaalen (review coordinator)[19], Philippe B. Bertrand[20], Natasja de Groot[21], Nicolas Derval[22], Maxim Didenko[23], Erwan Donal[24], Marc R. Dweck[25], and Siew Yen Ho[26,27]

[1]Arrhythmia Section, Department of Cardiology, Hospital Clínic, University of Barcelona, Carrer Villarroel 170, Barcelona 08036, Spain; [2]Department of Cardiology, Angiology and Intensive Care Medicine, German Heart Center of the Charité (DHZC), Charitéplatz 1, Berlin 10117, Germany; [3]Biosciences Institute, Centre for Life, Newcastle University, Newcastle-upon-Tyne NE1 3BZ, UK; [4]Department of Cardiology, University Hospital Heidelberg, Im Neuenheimer Feld 410, Heidelberg 69120, Germany; [5]Institute of Biomedical Engineering, Computational Cardiac Modeling, Karlsruhe Institute of Technology (KIT), Fritz-Haber-Weg 1, Karlsruhe 76131, Germany; [6]William Harvey Research Institute, NIHR Barts Biomedical Research Centre, Queen Mary University London, Charterhouse Square, London EC1M 6BQ, UK; [7]Barts Heart Centre, St Bartholomew's Hospital, Barts Health NHS Trust, West Smithfield, London EC1A 7BE, UK; [8]Department of Cardiology, Radboud University Medical Center, Geert Grooteplein Zuid 10, Nijmegen 6525 GA, The Netherlands; [9]Department of Radiology, Medical Imaging Centre, Semmelweis University, 2 Korányi Sándor St, Budapest 1083, Hungary; [10]Department of Cardiology, Leiden University Medical Center, Albinusdreef 2, Leiden 2333 ZA, The Netherlands; [11]Department of Electrical, Electronic and Information Engineering 'Guglielmo Marconi', University of Bologna, Viale del Risorgimento, 2, Bologna, BO 40136, Italy; [12]Johns Hopkins All Children's Hospital, Heart Institute, St Petersburg, FL, USA; [13]Departamento de Anatomía Humana y Biología Celular, Facultad de Medicina, Universidad de Extremadura, Badajoz, Spain; [14]COR Group, ITACA Institute, Universitat Politècnica de València, Camí de Vera, s/n, València 46022, Spain; [15]Department of Computer Science, British Heart Foundation Centre of Research Excellence, University of Oxford, Oxford OX1 3QG, UK; [16]Department of Physiology, Cardiovascular Research Institute Maastricht, Maastricht University, PO Box 616, Maastricht 6200 MD, The Netherlands; [17]Cardiology Department, Hospital Universitario Quirónsalud Madrid, European University of Madrid, c/ Diego de Velázquez, 1, Madrid 28223, Spain; [18]Arrhythmia and Robotic EP Unit, La Paz University Hospital, P. Castellana, 261, Hospital General La Paz, Madrid 28046, Spain; [19]Department of Cardiology, Leiden University Medical Center, Leiden, The Netherlands; [20]Department of Cardiology, Ziekenhuis Oost-Limburg, Genk, Belgium; [21]Department of Cardiology, Erasmus University Medical Center, Rotterdam, The Netherlands; [22]IHU LIRYC, Electrophysiology and Heart Modeling Institute, Cardiac Electrophysiology and Stimulation Department, Fondation Bordeaux Université and Bordeaux University Hospital (CHU), Pessac-Bordeaux, France; [23]Clinic for Electrophysiology and Rhythmology, Heart and Diabetes Center North Rhine-Westphalia, University Hospital of Ruhr University Bochum, Bad Oeynhausen, Germany; [24]CHU Rennes, University of Rennes, Inserm, LTSI—UMR 1099,

* Corresponding author. Tel: +493 045 051 3142; fax: +4 930 450 751 3932. *E-mail address*: althoff.tf@gmail.com; Twitter: @TillAlthoff

Rennes F-35000, France; [25]BHF Centre for Cardiovascular Science, University of Edinburgh, Little France Crescent, Little France, Edinburgh EH16 4SB, UK; [26]Cardiac Morphology, Royal Brompton Hospital, London, UK; and [27]National Heart & Lung Institute, Imperial College London, London, UK

Received 9 May 2025; accepted after revision 20 June 2025; online publish-ahead-of-print 30 July 2025

Abstract

This clinical consensus document proposes standardized atrial segments for 3D imaging, electroanatomical mapping and computational modelling, based on anatomical, electrophysiological and clinical considerations, with precise definitions of regional borders allowing for reproducible and automated regionalization. 3D imaging and high-resolution electroanatomical mapping have become an integral part of cardiac electrophysiology and the management of patients with arrhythmias. However, to perform regional quantitative analyses and intra- and inter-individual, as well as cross-modality comparisons, a universal definition of atrial regions and their boundaries is required. While for the left ventricle there is already an established standardized regionalization (AHA 17-segment model), there is no such consensus for the atria. In a multi-disciplinary writing group consisting of cardiologists, cardiac electrophysiologists, cardiovascular imaging specialists, and anatomists as well as specialists in computational cardiac modelling from European Heart Rhythm Association and European Association of Cardiovascular Imaging, a standardized regionalization based on a 15-segment bi-atrial model was elaborated. This clinical consensus document will enable consistent regional analyses and homogeneous data acquisition across different centres and modalities, and may thus have a significant impact on atrial arrhythmia research and personalized treatment approaches based on individual arrhythmia patterns and phenotypes.

Graphical Abstract

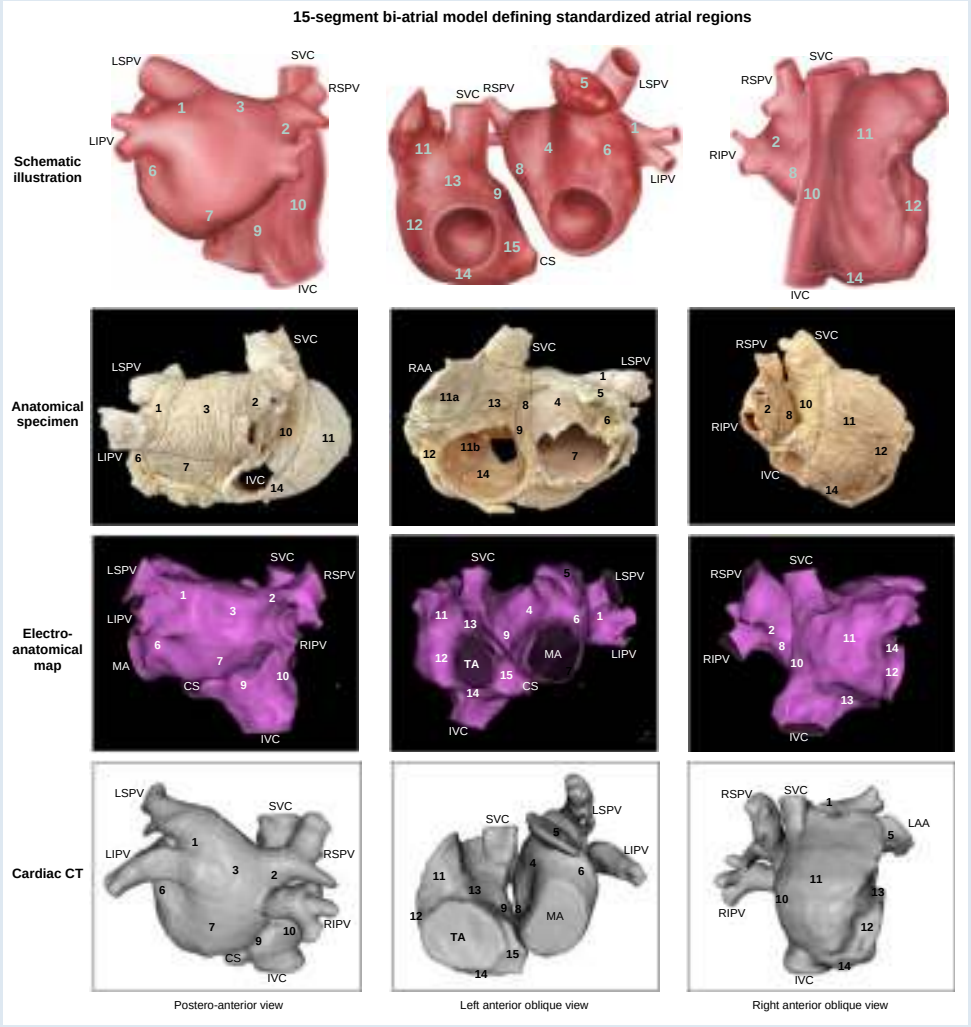

Keywords

Atrial regions • Segmentation • Cardiac imaging • Electroanatomical mapping • Atrial fibrillation • Catheter ablation

Table of contents

What's new?

- While for the left ventricle there is already an established standardized regionalization (AHA 17-segment model), there is no such consensus for the atria. We are presenting a standardized regionalization of the cardiac atria for 3D imaging, electroanatomical mapping, and computational modelling.
- The regionalization in this 15-segment bi-atrial model is based on anatomical, electrophysiological, and clinical considerations.
- Reproducibility and universal applicability were validated by use of two software algorithms independently developed for automatic regionalization.
- Developed in a multi-disciplinary writing group consisting of cardiologists, cardiac electrophysiologists, cardiovascular imaging specialists, and anatomists as well as specialists in computational cardiac modelling, the model enables consistent regional analyses and homogeneous data acquisition across different centres and modalities.
- The 15-segment bi-atrial model may thus facilitate the employment of digital health- and artificial intelligence-based approaches and have a significant impact on personalized arrhythmia therapies.

Introduction

Three-dimensional (3D) imaging and high-resolution electroanatomical mapping have become an integral part of cardiac electrophysiology and the management of patients with arrhythmias.[1,2] With further technological advances, the significance of these and other 3D modalities continues to grow.[3,4] Today, the spatial resolution of the various modalities

allows for accurate regional characterization of morphological and electrophysiological properties.[5–10] To perform regional quantitative analyses, however, as well as intra- and inter-individual and cross-modality comparisons, a universal definition of atrial regions and their boundaries is required. Such universal definition will foster consistent regional analyses and promote homogeneous data acquisition across different centres and modalities. This will in turn facilitate the employment of digital health- and artificial intelligence-based approaches.[11]

While a standardized regionalization of the left ventricle has been produced by the American Heart Association in their 17-segment model, which is widely accepted and routinely applied, there is no such consensus for segmentation of the atrial chambers.[12] The regionalizations previously described in the literature for the atrial chambers did not aim for universal applicability, but were rather created to accommodate the distinct demands of the specific analysis.[13–16] Moreover, the existing definitions for the atrial regions are not sufficiently precise to allow for reproducible regionalization.[17–19]

Scope of the document

This clinical consensus statement is a joint effort from the European Heart Rhythm Association (EHRA) and the European Association of Cardiovascular Imaging (EACVI) of the European Society of Cardiology (ESC) based on an initiative of the European Union—Marie Skłodowska-Curie Actions Doctoral Network 'PersonalizeAF'. It aims to segment atrial regions in a consistent manner across imaging, electroanatomical mapping and computational modelling techniques, defining their borders with sufficient precision to permit reproducible and automated regionalization. Recognizing the current limitations in spatial resolution provided by existing clinical modalities, the proposed model has been designed to balance the evident trade-off between universal applicability on the one hand, and anatomical accuracy on the other hand.

Methods

European Society of Cardiology scientific document policy

The clinical consensus statement was approved by the ESC Scientific Document Committee and the ESC Clinical Practice Guidelines Chair.[20]

Writing committee

The EHRA, as the leading association, nominated the chair of the document. The writing committee was defined based on a list of representatives put forward by each of the two associations involved (EHRA and EACVI). It consisted of a multi-disciplinary group of cardiologists, cardiac electrophysiologists, cardiovascular imaging specialists, and anatomists as well as specialists in computational cardiac modelling.

All members provided disclosure statements to assess potential conflicts of interest.

General approach

Existing evidence was evaluated based on a comprehensive literature search in Medline (via PubMed), in accordance with applicable guidelines.[20,21] Subsequently, the writing group held face-to-face meetings and web-based conference calls to establish standardized atrial regions which can be universally linked to 3D atrial geometries as derived from imaging, electroanatomical mapping, or computational modelling. The regions were defined based on anatomical, electrophysiological, and clinical considerations, taking into account the limitations in spatial resolution of some of the modalities. Definitions of the borders had to be sufficiently precise to enable reproducible and automated regionalization. Universal applicability and reproducibility of the proposed regions was validated in an unbiased manner using two independent software algorithms for automatic regionalization, which were developed by members of the writing group.[22,23]

The degree of agreement among the co-authors was evaluated for each of the 15 atrial segments in a survey. During voting, each member had the option to agree, disagree, or abstain. Modifications were made based on raised comments. The final approval rate was 100% for each of the proposed regions without any abstentions.

Auxiliary points and planes

Depending on the modality used for imaging or mapping, the spatial resolution may not be sufficient to define all atrial segments based exclusively on anatomical landmarks or morphological features. Thus, wherever adequate anatomical landmarks were lacking, auxiliary points and planes were created to help define regional borders. These points and planes may appear somewhat arbitrary. They were introduced to permit automated regionalization and reproducible definition of the selected atrial segments, thus promoting the required standardization and universal applicability.

Standardized axes and nomenclature

Standardized axes and their corresponding projections, as well as universally acceptable terminology are required to ensure precise and reproducible regional definitions. The definitions and terminology suggested for the proposed model are based on the attitudinal body axes as well as the cardiac axes, and they are in accordance with the Consensus Statement from the Cardiac Nomenclature Study Group of the ESC (*Figure 1*).[24–28]

Attitudinal body axes

Attitudinal body axes are based on trans-axial or body-plane orthogonal projections and define planes and axes that are parallel or at right angles to the longitudinal axis of the body. These projections imply standard directional terms based on the orientation of the human body, such as anterior or ventral as opposed to posterior or dorsal, and superior or cranial as opposed to inferior or caudal (*Figure 1A*).

Cardiac axis

While the attitudinally appropriate planes and their projections permit the cardiac components to be described during life as they are assessed within the body, definitions based on the axis of the heart itself can be more appropriate when assessing certain atrial components and regions. Our model, therefore, also uses as an additional reference the longitudinal axis of the heart, from its base to its apex, which is orthogonal to the planes of the mitral and tricuspid valves (*Figure 1B*). The American Heart Association Scientific Statement on Standardized Myocardial Segmentation and Nomenclature for Tomographic Imaging of the Heart also defines the cardiac segments using the cardiac long axis and its corresponding orthogonal planes.[12]

The atrial septum, furthermore, is aligned along the cardiac long axis (see the directional indicator in *Figure 1B*). This means it is ideally suited not only to distinguish apical as opposed to basal directions in the longitudinal planes, but also septal and lateral directions in the short axis planes.[29] The right anterior oblique fluoroscopic projection, which represents an anteroposterior projection rotated around the longitudinal body axis by 30° to 45°, essentially corresponds with the cardiac long axis.

Clock model

In addition to our use of auxiliary points and planes based on standardized axes, we also use a clock model to facilitate the definition of distinct features of the left and right atrioventricular junction (*Figure 2*). We defined the model using an anterior view of the plane containing the left and right atrioventricular junctions, representing the junctions as perfect circles. This plane is orthogonal to the long cardiac axis, which as we have explained corresponds to a left anterior oblique fluoroscopic projection when rotated through between 45° and 60° around the longitudinal body axis. When using the model, the superior 12 o'clock and inferior 6 o'clock positions are marked by a vertical mid-line taken through the centre of the valvular orifices. More precisely, the vertical 12 o'clock vector is defined as the orthogonal projection of the longitudinal body axis (pointing upwards) onto the plane of the left and right atrioventricular junction, respectively. The 12 o'clock and 6 o'clock positions then correspond with 0° and 180° relative to the circle, with every hour representing 30°.[15]

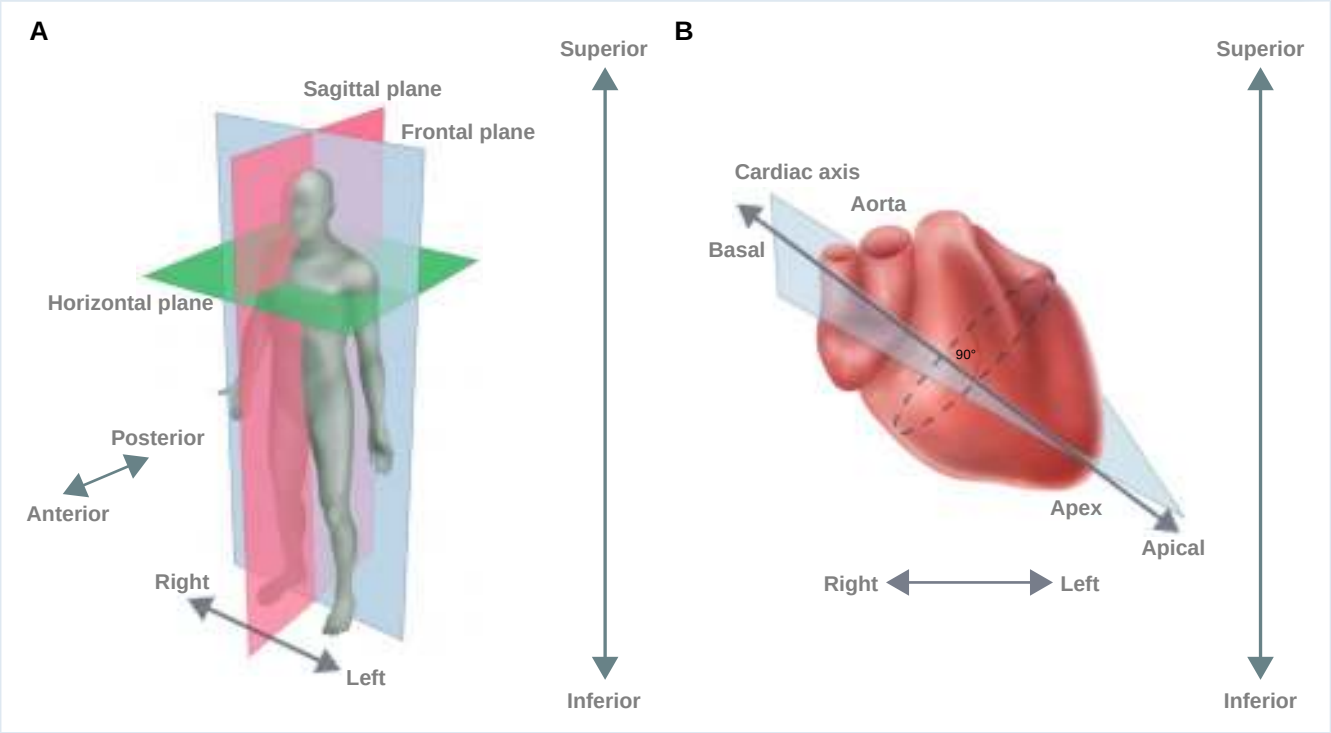

Figure 1 Standard axes and planes. (*A*) Body axes and corresponding planes. Directions are indicated according to the standard attitudinal terminology, with anterior, posterior, superior, inferior, left and right corresponding to ventral, dorsal, cranial, caudal, left and right direction, respectively. (*B*) Cardiac axis and corresponding planes. The cardiac axis is defined by the line connecting the aortic root and cardiac apex. The cardiac axis indicates the apical and basal direction, respectively.

Geodesics

So as to define regional boundaries themselves insufficiently defined by detectable anatomical features, and to ensure reproducibility and standardization, we have used the concept of geodesics. A geodesic represents the shortest path on the atrial surface between two defined points, irrespective of whether the points themselves represent known anatomical landmarks or auxiliary entities.

Specific structures

When defining the atrial segments, we have not recognized known anatomical entities of functional or electrophysiological relevance, such as Bachmann's bundle, the oval fossa or the Eustachian valve. If required, and if their location can accurately be determined using clinical modalities, their locations can be superimposed onto the regions we have defined.

Background—development and gross anatomy of the atrial chambers

Developmental considerations

Thanks to our recent advances in the understanding of cardiac development in the human heart, we are now able to recognize the various components that join together during the embryonic and foetal periods to produce the definitive atrial chambers (*Figure 3*).[30] These findings, in turn, permit us to recognize the anatomically discrete areas within the post-natal organ.

An atrial component of the developing heart can be recognized during the initial stages of, looping of the primary heart tube. This primary component becomes the bodies of both atrial chambers, albeit with the larger part committed to the left atrium (*Figure 3*). A process of so-called 'ballooning' then forms the atrial appendages. The walls of these new components are made up of chamber myocardium, although eventually all of the cardiomyocytes within the atrial walls, apart from those forming the sinus and atrioventricular nodes, become working cells. The transfer of the developing systemic venous sinus, or 'sinus venosus', to the right side of the primary atrial component reflects the development of anastomotic channels such that the venous returns from the placenta, yolk sac, and the embryo itself, initially symmetrical, become dominant on the right side. When the primary atrial septum begins to separate the primary atrial part of the heart tube, it is then able to grow towards the atrioventricular canal such that the systemic venous tributaries are to its right side. At the same time, the atrioventricular canal myocardium becomes incorporated into both developing atrial chambers as their vestibules (*Figure 3*).

The commitment of the pulmonary veins to the developing left atrium is a later event. A mid-line strand initially connects the venous channels developing within the lung buds with the atrial cavity. Having canalized, the new pulmonary vein enters the primary atrial component through the dorsal mesocardium. Growth of the primary atrial septum towards the atrioventricular canal places it to the left of the initial solitary pulmonary venous orifice, which opens adjacent to the vestibule. Muscularization of a pharyngeal mesocardial outgrowth, known as the vestibular spine, along with a mesenchymal cap carried on the leading edge of the primary atrial septum, then forms the second atrial septum. Remodelling such that four pulmonary veins enter the venous sinus at its corners is not completed until the foetal stages of development. With the remodelling, the pulmonary venous component forms the superior wall of the left atrium, or its dome. The superior margin of the oval foramen can then be seen to be an infolding of the atrial walls (*Figure 3*).

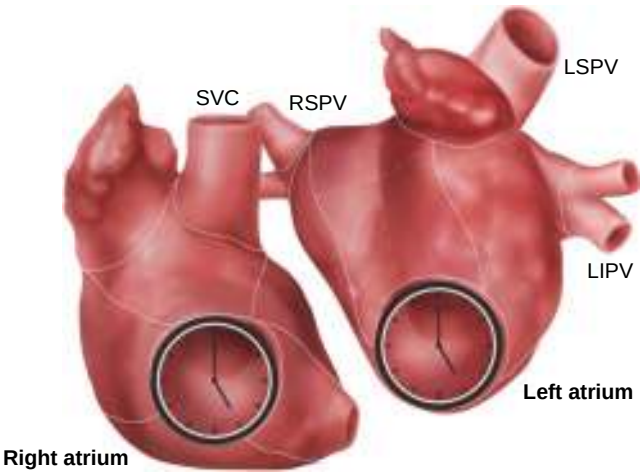

Figure 2 Clock model indicating specific locations at the left and right atrioventricular junction in a left anterior oblique view. SVC, superior caval vein; RSPV, right superior pulmonary vein; LSPV, left superior pulmonary vein; LIPV, left inferior pulmonary vein.

Right atrium

Knowledge of the developmental processes described above now underscores the appropriate description of the definitive morphology of the atrial chambers. The initial atrial component of the primary heart tube persists as the bodies of both atriums, but post-natally very little of the body can be recognized within the morphologically right atrium. The right atrial morphology is dominated by the extensive walls of its appendage, which can be recognized by virtue of the presence of the pectinate muscles on their endocardial surface (*Figure 4A*). The pectinated appendage forms the entirety of the lateral atrial wall, with the pectinate muscles themselves extending all around the smooth-walled vestibule. The boundary between the pectinated appendage and the systemic venous sinus is marked postero-laterally by the prominent terminal crest, or 'crista terminalis'. Opening into the venous sinus are the superior and inferior caval veins, with remnants of the embryonic right venous valve usually persisting at the mouths of the inferior caval vein and coronary sinus as the Eustachian and Thebesian valves. The leftward boundary of the venous sinus is rarely obvious, but on occasion it is marked by persistence of the left venous valve. When present, this permits recognition of the atrial body as the space between the remnants of the left venous valve and the atrial septum (*Figure 3*). The septal aspect of the chamber, at first sight, is extensive (*Figure 4A*). In reality, only the floor of the oval fossa and its antero-inferior buttress are true septal structures that interpose directly between the cavities of the right and left atriums. The remainder of the rims of the oval fossa are infoldings of the atrial walls, as is the ridge between the orifices of the inferior caval vein and the coronary sinus, with this structure often described as the sinus septum. It is better considered as the Eustachian ridge. The commissure of the Eustachian and Thebesian valves runs through this ridge as the tendon of Todaro, forming one of the landmarks of the important triangle of Koch (*Figure 4B*).[31] The equally important cavotricuspid isthmus is found inferior to the base of the triangle, with the vestibule between the orifice of the coronary sinus and the hinge of the septal leaflet of the tricuspid valve producing a septal isthmus (*Figure 4B*).[32]

Left atrium

In contrast to the morphologically right atrium, which has predominantly pectinated walls belonging to the appendage, the majority of the walls of the morphologically left atrium are smooth (*Figure 5A*). This makes it harder to recognize its developmental components.

The appendage, nonetheless, which again has pectinated walls, is obvious as a tubular outpouching from the anterior part of its cavity. The pulmonary venous component can also be recognized as forming the superior wall, well described as the atrial dome, with an obvious ridge on its lateral wall marking the entrance of the left-sided pulmonary veins. The veins on each side join the pulmonary venous component through the antrums. The pulmonary veins themselves then extend from the antrums on each side towards the hilums. The proximal walls of the veins are myocardial, producing the pulmonary venous myocardial sleeves which, at the margins of the pericardial cavity, merge with the walls of the extrapericardial veins, which are made up of smooth muscle. There are usually two myocardial sleeves on each side, but there is individual variation, varying from three discrete sleeves to the presence of a common sleeve extending to the margins of the pericardial cavity.[33]

The remainder of the walls of the left atrium are made up of the smooth-walled vestibule and the atrial body. It is these parts that form the posterior wall of the chamber. Whereas, the rims of the oval fossa represent the septal landmarks in the right atrium, it is the flap valve of the oval fossa, derived from the primary atrial septum, that is seen on the left side. It possesses two obvious horns where it overlaps the infolded walls forming the superior margin of the fossa (*Figure 5A*). Significant isthmuses are found in the lateral wall of the atrium, with the mitral isthmus present between the openings of the left pulmonary veins and the hinge of the mural leaflet of the mitral valve (*Figure 5B*). A second, narrower, isthmus can then be recognized more anteriorly between the orifice of the left atrial appendage and the hinges of the mitral valvular leaflets at the atrioventricular junction.[34,35]

Atrial regionalization (15-segment bi-atrial model)

Segmentation of the left atrium

Segments 1 and 2: the left and right pulmonary venous antrums

Anatomical, electrophysiological, and clinical considerations

The walls of the venous antrums are distinct atrial regions that produce the transition from the myocardial walls of the left atrium itself to the

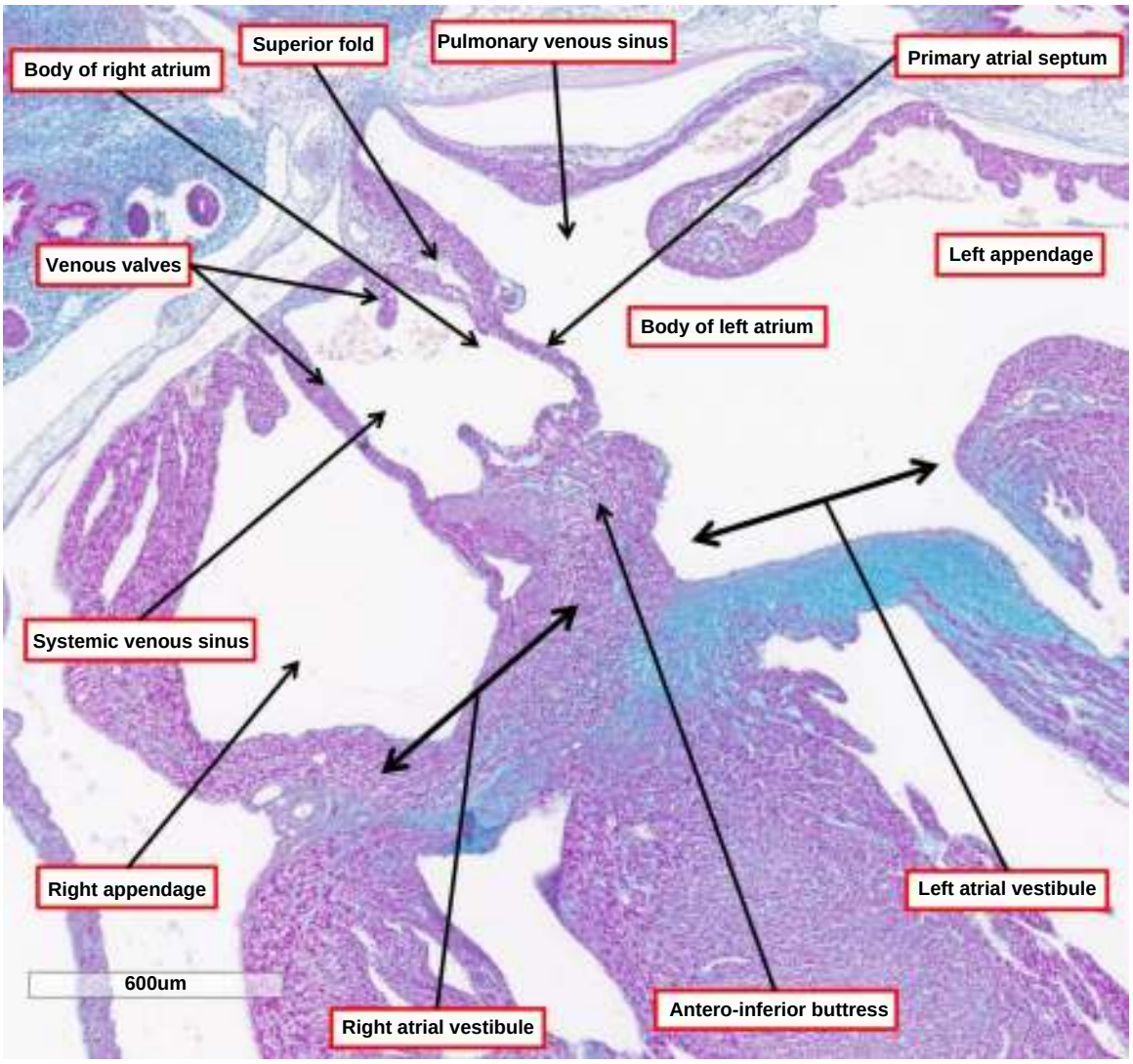

Figure 3 The image is a frontal section through the atrial chambers of a human foetus at 9 weeks of development. It is possible to recognize the developmental origins of the components of both atrial chambers. Each atrium possesses a body, which is the remains of the atrial component of the primary heart tube. The vestibules are derived from the atrioventricular canal myocardium of the primary tube. The appendages are chamber myocardium, formed by the process of ballooning from the body on each side. Each atrium now possesses its venous sinus, with the venous valves still recognizable to show the boundaries of the systemic venous sinus of the right atrium. The primary atrial septum forms the floor of the oval fossa, with its antero-inferior buttress formed by muscularization of the vestibular spine and mesenchymal cap of the primary septum. The superior margin of the fossa is clearly seen to be an infolding between the atrial walls.

smooth muscular walls of the extrapericardial pulmonary veins. Forming segments 1 and 2 of our 15-segment bi-atrial model, the myocardial pulmonary venous sleeves extend distally from the body of the atrial cavity, with the body itself roofed by the atrial dome, which we will describe as segment 3. It is at the distal margins of the venous sleeves that the walls transition to be formed by smooth muscle rather than working myocardium.[27,35–38]

The interplay between the working cardiomyocytes and the smooth muscle cells at the distal venoatrial junctions is believed to underscore the specific electrophysiological properties that are now known to play an important role in the pathogenesis of atrial fibrillation and other atrial arrhythmias.[39,40] It is this knowledge, in turn, which supports the circumferential ablation of the antrums, thus producing the electrical isolation of the pulmonary veins, which constitutes the cornerstone of current treatment of atrial fibrillation.[2,41]

While there are typically two pulmonary veins on each side entering their respective antrums, it is not infrequent to find variations, such as three venous orifices, or the pulmonary veins entering the antrums through a common orifice, often described as 'common trunk'.[27,35–38]

Definition of segmental boundaries

Anteriorly, the left antrum is bordered by the left lateral ridge, part of the lateral wall of the atrial body, which is defined as segment 6. Posteriorly, the proximal border can be appreciated as a sudden change in the curvature at the morphological transition from the antrum to the atrial dome (*Figures 6* and *7*).

When defining the border by mathematical algorithms, the junction of the antrum with the atrial body may be recognized as a discontinuity in the curvature function. This could be an inflection point where the

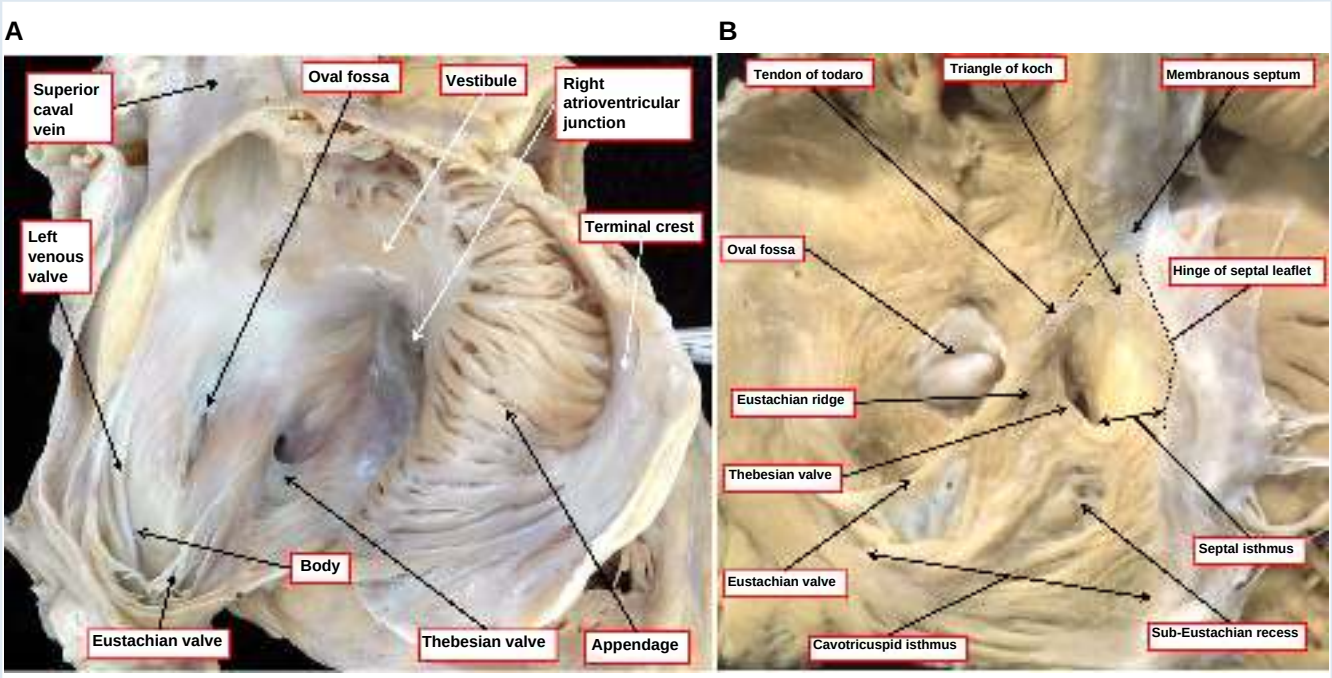

Figure 4 Gross anatomy of the right atrium. (*A*) The morphologically right atrium has been opened by making an incision within the systemic venous sinus parallel to the terminal groove, and reflecting the appendage laterally. The heart is viewed from a lateral projection that corresponds to a right posterior oblique view. It is possible to recognize all the anatomical components that make up the atrial chamber. The appendage is characterized by its pectinated walls. The smooth vestibule separates the appendage from the hinges of the leaflets of the tricuspid valve in the right atrioventricular junction. The remnants of the embryonic right venous valve, seen as the Eustachian and Thebesian valves guarding the mouths of the inferior caval vein and coronary sinus respectively, delineate the lateral border between the venous sinus and the appendage. In this heart, the remnant of the left venous valve can also be seen, making it possible to recognize the small part of the atrial body interposed between the valvular remnants and the septal surface. The depression on the septal surface shows the location of the true septum. It is not possible to identify the paraseptal areas. (*B*) The image shows the en-face septal aspect of the cavity of the morphologically right atrium. The endocardium has been removed to show the 'grain' produced by the parallel aggregation of the individual cardiomyocytes. It is possible to recognize the rims and floor of the oval fossa. Only the area adjacent superior to the tendon of Todaro is a true second septal component over and above the flap valve forming the floor of the fossa. The dissection also shows the boundaries of the triangle of Koch along with the locations of the cavotricuspid and septal isthmuses.

curvature changes sign (from concave to convex, or the other way round), or a turning point where the gradient of the curvature changes sign and the derivative of the curvature function turns to zero. The change in curvature is quite pronounced at the transition towards the left lateral ridge, representing the anterior border. Posteriorly, however, at the transition towards the atrial dome, which is part of segment 3, the change in curvature may be subtle.

Reproducibly to define the left pulmonary venous antrum as designated by segment 1, the change in the 2D curvature, indicating the junction, can be marked superiorly at point A, and inferiorly at point B, with these points representing the transitions towards the atrial body. These features are best appreciated in an attitudinal postero-anterior projection, which provides an en-face view of the atrial dome. By definition, in this view the uppermost part of an anatomical structure corresponds to its most superior or cranial, aspect as defined by the longitudinal body axis. The lowermost refers to its most inferior, or caudal, aspect.

The proximal border of the mouth of the left antrum is then delineated by the geodesic connecting points A and B, with the border at the same time encircling the antrums and orifices of the left inferior and superior pulmonary veins (see *Figure 7*). When traced distally, the antral region is bordered by the orifices of the left inferior and superior veins, respectively.

Except for those individuals having a common proximal venous myocardial sleeve, the sleeves of the superior and inferior pulmonary veins are separated by the venous carina. In those with three venous orifices, there will be two carinas.

As was the case for the left pulmonary venous antrum, the junction of the right pulmonary venous antrum and the atrial body can be recognized as a sudden change in the curvature indicating the morphological transition.

Reproducibly to define the right pulmonary venous antrum as designated by segment 2, the change in the 2D curvature indicating the junction can be marked by points C and D, representing the transitions towards the atrial body. As outlined above, these are best recognized in an attitudinal, postero-anterior projection. The proximal border of the antral mouth is then delineated by the shortest circumference connecting points C and D, which encircles the antrum and the orifices of the right inferior and superior pulmonary veins (see *Figure 8*).

The right pulmonary venous antrum extends distally to the margins of the myocardium forming the sleeves of the individual pulmonary veins (*Figure 8*). As with the left antrum, apart from those individuals with a common pulmonary venous sleeve, a carina will separate the sleeves of the right superior and inferior pulmonary veins.

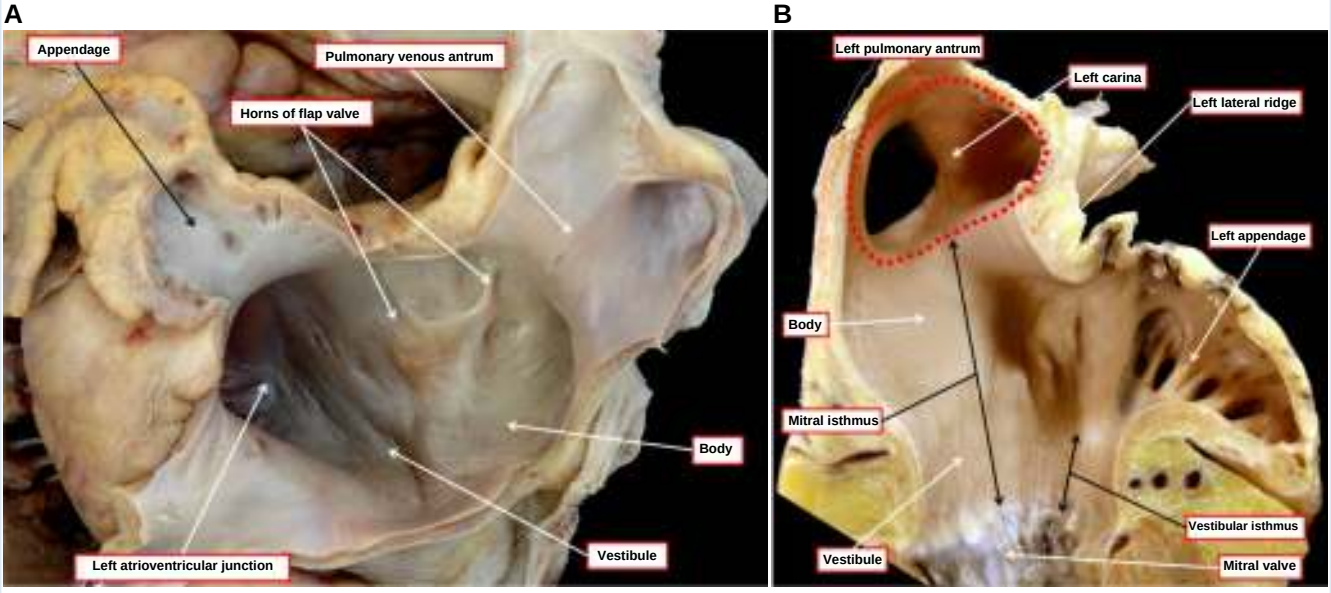

Figure 5 Gross anatomy of the left atrium. (*A*) The morphologically left atrium from the same heart as used to prepare *Figure 4* has been opened by making cuts in its lateral wall, and reflecting the wall to show its cavity. It is possible to recognize the tubular appendage by virtue of the pectinated nature of its walls. The remaining walls are all smooth, but these are made up of the vestibule, the body, and the pulmonary venous component. Note that the venous component forms the superior wall of the chamber, or its dome. The posterior wall is made up of the body and the vestibule. The flap valve of the septum is adherent to the rims of the oval fossa, better seen from the right side (*A*). It is possible to recognize the myocardial sleeves of the left pulmonary veins, which come together to form the left pulmonary venous antrum. The orifices of the right antrum cannot be seen. Note the coronary sinus within the inferior atrioventricular groove. (*B*) The image shows the lateral wall of the morphologically left atrium as viewed from the septal aspect. The superior and inferior pulmonary veins are seen entering the left antrum of the venous sinus, separated by the venous carina. The left lateral ridge, part of the body of the atrium, interposes between the orifices of the left pulmonary veins, and the mouth of the appendage. It is possible to recognize the mitral isthmus, between the pulmonary venous orifices and the hinge of the mural leaflet of the mitral valve, and the second, narrower, isthmus formed between the mouth of the left appendage, and the hinge of the mitral valvular leaflet. The latter isthmus is formed by the atrial vestibule, whereas both the vestibule and the lateral wall of the body of the atrium make up the mitral isthmus.

Segment 3: left atrial posterior wall (including sub-segments 3a, 3b, 3c, and 3d)

Anatomical, electrophysiological, and clinical considerations

The segment referred to as 'posterior wall' by cardiologists and electrophysiologists, is not strictly posterior but also has superior aspects.[42] In fact, anatomically this segment may be better described as the left atrial dome.[27,35,37] It shares a common embryologic origin with the pulmonary venous myocardial sleeves including an association with epicardial parasympathetic ganglia.

The myocardial walls of the dome have distinct electrophysiological properties that may predispose to conduction delay. It frequently harbours fibrotic arrhythmogenic substrates.[13,43,44] The left atrial posterior wall, therefore, is a common target should catheter ablation be considered over and above the isolation of the venous antrums, albeit supportive evidence from large randomized trials is lacking to date.[42,45] Recent analyses suggest that patients selected based on individual arrhythmogenic substrate might benefit from posterior wall isolation.[15,46]

Moreover, the dome contains the septopulmonary bundle, which consists of epicardial fibres that originate from the septum and span over the posterior wall towards the vestibule. Epicardial bridging via the septopulmonary bundle and endocardial breakthrough may impede successful posterior wall isolation by endocardial catheter ablation.[47,48]

So as to accommodate the considerable regional differences in atrial remodelling, the dome may be further divided into quadrants. Fibrotic remodelling, as detected by late gadolinium enhancement cardiac magnetic resonance, occurs predominantly in the left lower posterior quadrant, which is adjacent epicardially to the descending aorta.[43,44,49,50]

Definition of segmental boundaries

Laterally and septally, segment 3 is bordered by the proximal boundaries of the venous antrums. These borders are best appreciated in an attitudinal postero-anterior projection, which provides an en-face view of the dome and also enables standardized definition of the superior and inferior borders (*Figure 9*). In this view, the uppermost part of the posterior wall corresponds to its most superior aspect, and the lowermost to its most inferior aspect. This means that the superior border, also referred to as the left atrial roof line, can be defined by the geodesic connecting points A and C, which in turn represent the most superior aspects of the left and right antral boundaries. It then follows that the inferior border is defined by the geodesic connecting points B and D on the antral boundaries. This definition of the posterior wall is consistent with the definition used in seminal studies including the CAPLA randomized trial.[42]

When considering division of the posterior wall into sub-segments, the superior and inferior quadrants may be divided by a geodesic bisecting the carinas. In those patients with a common venous orifice ('common trunk'), or additional orifices, it may be more appropriate to use a horizontal geodesic, which bisects the lateral and septal borders of the

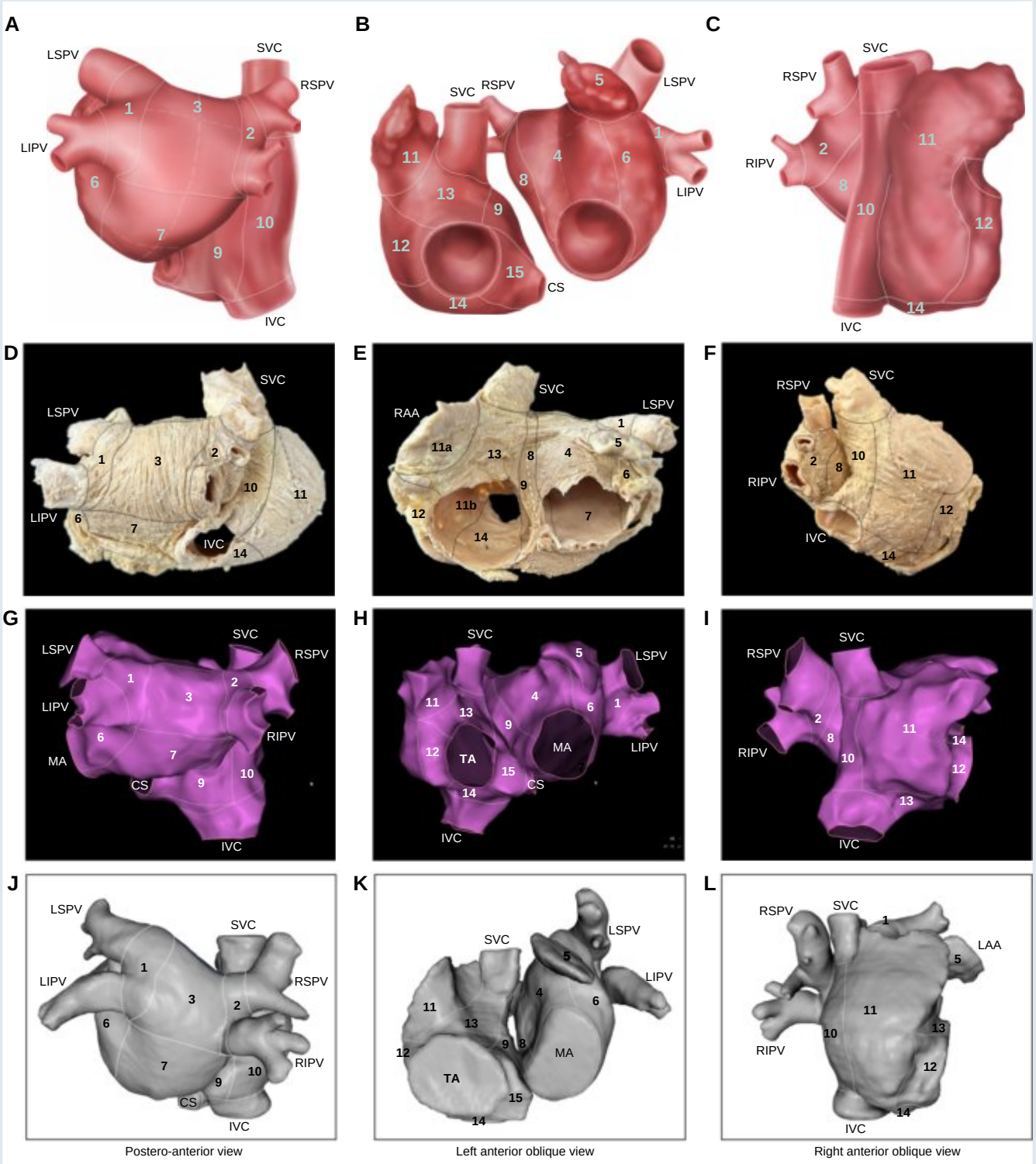

Postero-anterior view | Left anterior oblique view | Right anterior oblique view

Figure 6 (Central illustration): 15-segment bi-atrial model. Illustrated visualization of the 15 left and right atrial segments in different views (*A–C*), and head-to-head comparison with anatomical sections (*D–F*) as well as electroanatomical mapping clinical routine CT-imaging (*G–I*) and electroanatomical mapping clinical routine CT-imaging (*J–L*) in the correspondent views. Left column: posterior-anterior view; middle column: left anterior oblique view; right column: right anterior oblique view. CS, coronary sinus; IVC, inferior vena cava; LAA, left atrial appendage; LIPV, left inferior pulmonary vein; LSPV, left superior pulmonary vein; MA, mitral annulus (left atrioventricular junction); RAA, right atrial appendage; RIPV, right inferior pulmonary vein; RSPV, right superior pulmonary vein; SVC, superior vena cava; TA, tricuspid annulus (right atrioventricular junction).

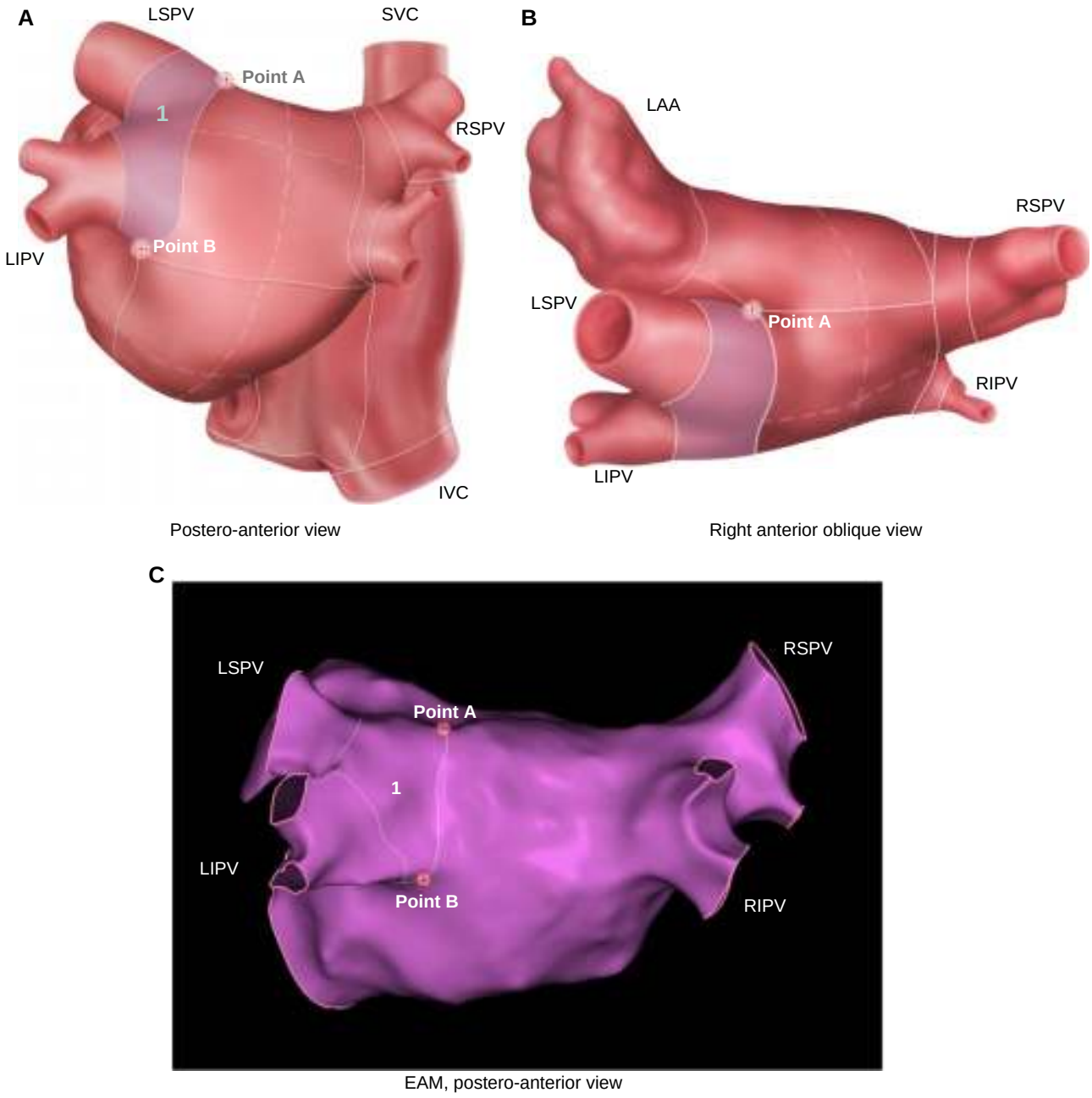

Figure 7 Segment 1 (left pulmonary antrum). Illustration of segment 1 in a postero-anterior view (*A*) and a superior view (*B*). (*C*) Clinical routine electroanatomical map visualizing segment 1 in a postero-anterior view. LSPV, left superior pulmonary vein; LIPV, left inferior pulmonary vein; RSPV, right superior pulmonary vein; RIPV, right inferior pulmonary vein.

posterior wall. The septal and lateral quadrants are divided by a horizontal bisecting line.

Segment 4: left atrial anterior wall (including sub-segments 4a, 4b, 4c, and 4d)

Anatomical, electrophysiological, and clinical considerations

The anterior atrial wall encloses the cavity representing the body of the left atrium, but also includes the vestibule, with the vestibular myocardium inserting into the part of the atrioventricular junction, which supports the aortic leaflet of the mitral valve. Bachmann's bundle runs through the superior part of the anterior wall. This aggregation of working atrial cardiomyocytes provides the principal pathway for interatrial conduction, extending as it does towards the lateral wall, or segment 6, and the left atrial appendage, or segment 5.[27,35,37,38] The anterior wall separates the atrial cavity from the aortic root and the ascending aorta. Its walls can be very thin.[29,37] Areas of low bipolar endocardial voltage, surrogates for arrhythmogenic substrates, are commonly encountered in this segment.[51,52]

Depending on the resolution of the modality being used for diagnosis, and the objective of the analysis, consideration can be given for dividing the anterior wall into quadrants. Division in this fashion may better account

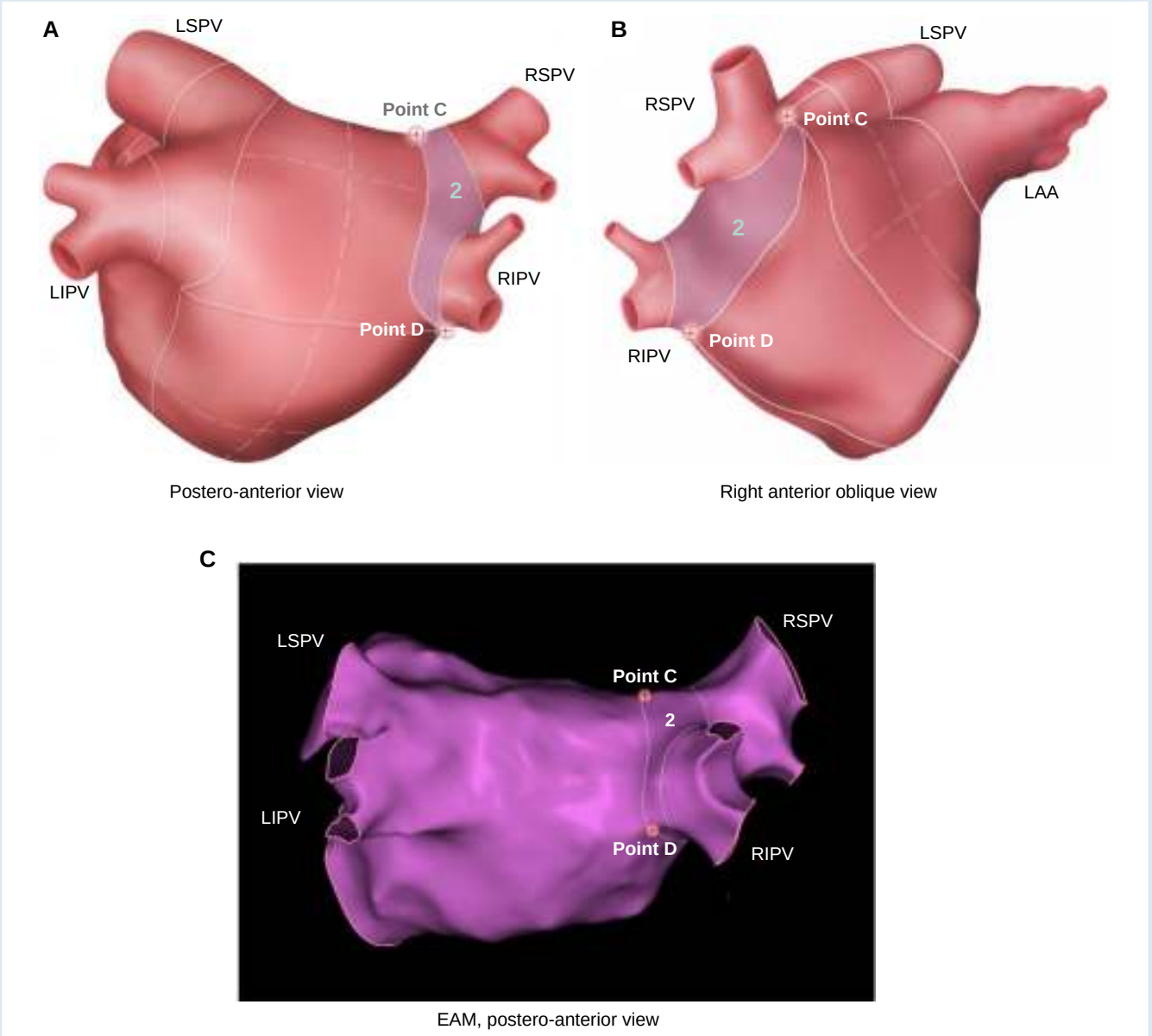

Figure 8 Segment 2 (right pulmonary venous antrum). Illustration of segment 2 in a postero-anterior view (*A*) and a right anterior oblique view (*B*). (*C*) Clinical routine electroanatomical map visualizing segment 2 in a postero-anterior view. RIPV, right inferior pulmonary vein; RSPV, right superior pulmonary vein; LIPV, left inferior pulmonary vein; LSPV, left superior pulmonary vein.

for the distinct regional distribution of arrhythmogenic substrates, which seems to be predominant in the baso-septal quadrant, anterior to the right superior pulmonary vein, itself directly adjacent to the ascending aorta.[51,52]

Definition of segmental boundaries

Segment 4 extends anteriorly and apically from the dome, ending in the part of the left atrioventricular junction, which supports the aortic leaflet of the mitral valve. The cranial boundary is defined by the roof line, already discussed in the context of segment 3. It is marked by the geodesic connecting points A and C (*Figure 10*). The apical border, at the left atrioventricular junction, is defined using an apico-basal view, which is parallel to the long cardiac axis and orthogonal to the plane of the mitral valve. As we have already emphasized, this view corresponds roughly to the left anterior oblique fluoroscopic projection. We have also explained how we use the clock model (*Figure 2*) to facilitate the definition of standardized and reproducible, albeit idealized, markers of the segmental borders. Based on this model, the apical border of the anterior wall, represented by point E, corresponds with 9 o'clock septally, and laterally with point F, found at 1 o'clock. The septal boundary is marked by the geodesic between the 9 o'clock position, or point E, and the intersection of the roof line with the right venous antrum, with the latter found at point C.

The basal part of the lateral border is defined by the shortest geodesic connecting the most superior aspect of the left antral boundary (point A), and the orifice of the left appendage. The intersection with the orifice of the appendage is then geodesically connected with the atrioventricular junction at 1 o'clock (point F) to define the apical

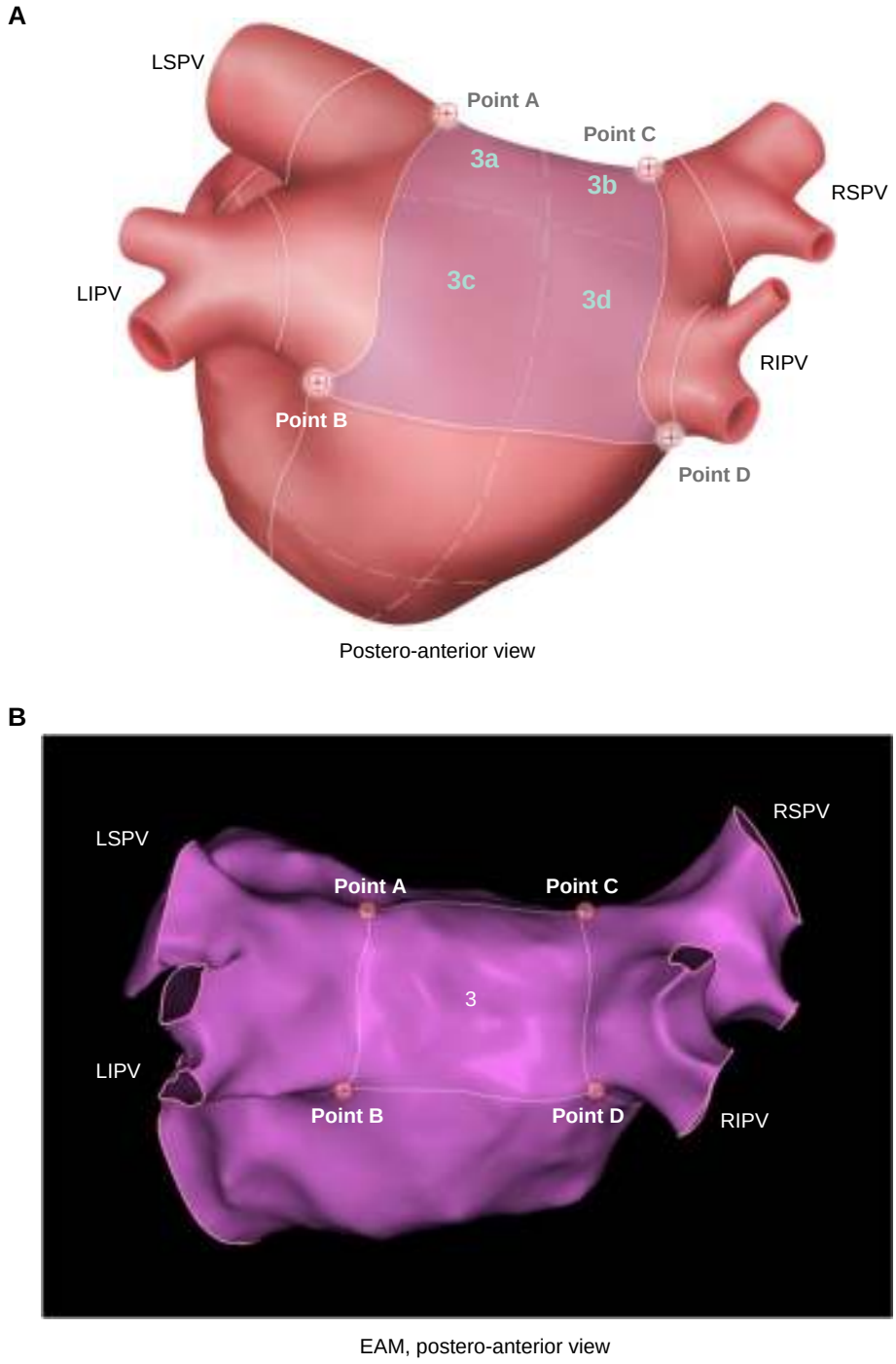

Figure 9 Segment 3 (left atrial posterior wall). Illustration of segment 3 in a postero-anterior view (*A*) and clinical routine electroanatomical map visualizing segment 3 in the same view (*B*). RIPV, right inferior pulmonary vein; RSPV, right superior pulmonary vein; LIPV, left inferior pulmonary vein; LSPV, left superior pulmonary vein.

part of the lateral border. Depending on the specific individual anatomy, the location of the appendage may interfere with the ability to place this geodesic. In such instances, the appendage should be ignored, and its orifice considered as part of the left atrial surface when seeking to create the geodesic. The orifice will only be considered as part of the atrial surface for the construction of the geodesic. It does not, of course, represent part of either the anterior or lateral wall segments.

As discussed, if necessary, the anterior wall can be sub-divided into quadrants. The basal, as opposed to the apical, quadrants can be defined by the geodesic that intersects the most anterior aspect of the orifice of the appendage and also bisects the septal border of the anterior wall (*Figure 10*). So as to differentiate the septal and lateral quadrants, the required geodesic bisects the roof line that itself sub-divides the basal and apical quadrants, and which extends

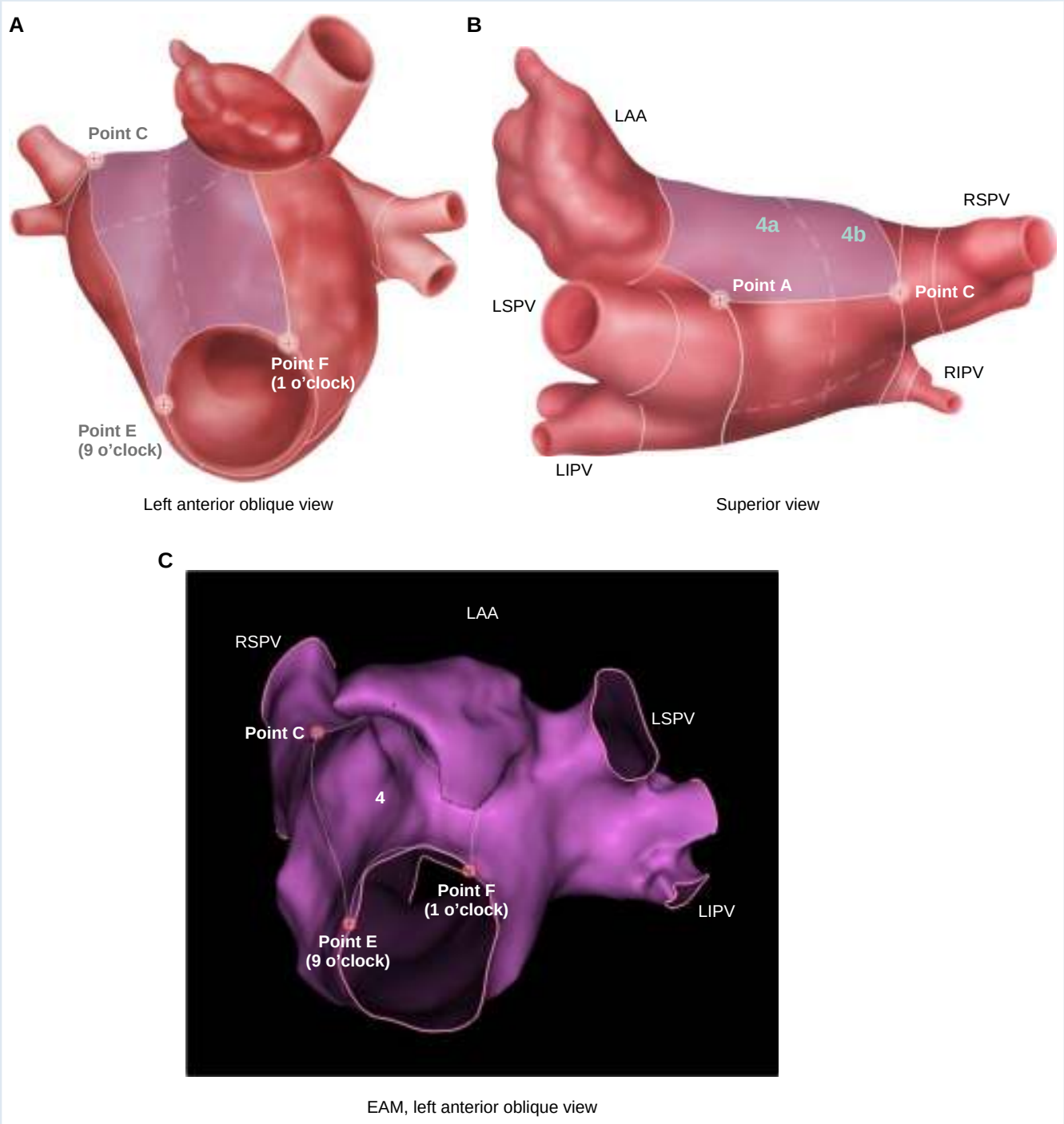

Figure 10 Segment 4 (left atrial anterior wall). Illustration of segment 4 in a left anterior oblique view (*A*) and a superior view (*B*). (*C*) Clinical routine electroanatomical map visualizing segment 4 in a left anterior oblique view. IVC, inferior vena cava; LAA, left atrial appendage; LIPV, left inferior pulmonary vein; LSPV, left superior pulmonary vein; RSPV, right superior pulmonary vein; SVC, superior vena cava.

apically to reach the left atrioventricular junction at the 11 o'clock position.

Segment 5: left atrial appendage

Anatomical, electrophysiological, and clinical considerations

The appendage is the tubular and angulated structure that protrudes from the atrial body. It can take very variable shapes, with multiple lobes and branches. Its wall is lined by pectinate muscles, being very thin between them. When compared with the right appendage, its mouth is constricted, and its junction with the atrial body limited.[27,29,33–38,53,54]

On account of its distinct morphology, and the resulting patterns of the flow of blood, it is a frequent site for the formation of intracardiac thrombus. Such formation of clot has been implicated in the aetiology of the cardioembolic strokes associated with atrial fibrillation.[55,56]

The enhanced automaticity observed in cardiomyocytes of the appendage, furthermore, has been implicated in the initiation and maintenance of atrial fibrillation.[13,57]

Definition of segmental boundaries

The appendage can readily be differentiated from the rest of the atrium by imaging or mapping. The cavity of its distal extremity shows a marked angulation with the remainder of the atrial cavity (*Figure 11*). In line with the concept introduced above, this junction can be recognized by the sudden change in the curvature at the morphological transition (see segment 1). Analogue to the junction of the antrum with the atrial body, the junction of the left atrial appendage with the atrial body may be recognized as a discontinuity in the curvature function. This would be a turning point where the gradient of the curvature changes sign and the derivative of the curvature function turn to zero.

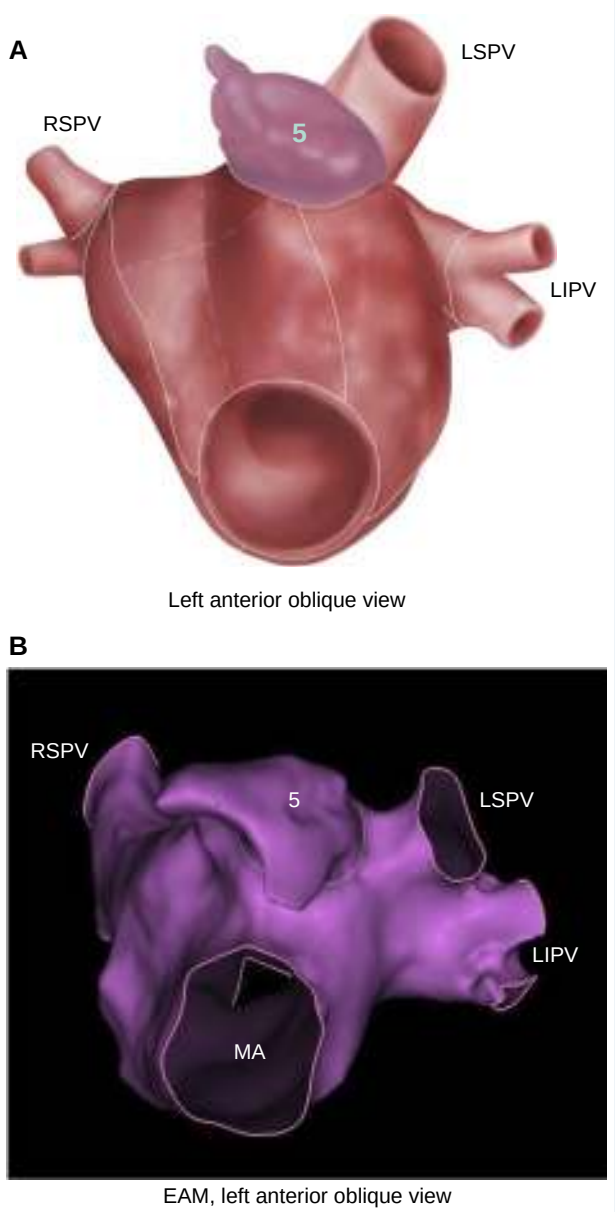

Figure 11 Segment 5 (left atrial appendage). Illustration of segment 5 in a left anterior oblique view (*A*) and a clinical routine electroanatomical map visualizing segment 5 in the same view (*B*). LIPV, left inferior pulmonary vein; LSPV, left superior pulmonary vein; MA, mitral annulus (left atrioventricular junction); RSPV, right superior pulmonary vein.

Segment 6: left atrial lateral wall (including sub-segments 6a and 6b)

Anatomical, electrophysiological, and clinical considerations

The lateral wall of the atrium, which makes up segment 6, comprises all lateral aspects of the atrial chamber aside from the left venous antrum. A prominent component of the wall is the left lateral ridge, which represents the lateral wall of the atrial body. It merges with the vestibule to separate the pulmonary venous antrum from the atrioventricular junction. This part of the lateral wall is the so-called mitral isthmus. The isthmus then extends apically as the vestibule, which separates the orifice of the appendage from the hinge of the leaflets of the mitral valve. The vestibular myocardium then continues to form the apical part of segment 6. The part of the ridge adjacent to the orifice of the appendage is often lined by extra-appendicular pectinate muscles, with the lateral wall itself being paper-thin between the individual muscles.[29,36,37]

Definition of segmental boundaries

Apically, the lateral wall is bordered by the lateral aspects of the left atrioventricular junction, which are marked by point F at 1 o'clock, and point H at 4 o'clock. The basal border is formed by the cranial margin of the left lateral ridge, separating the lateral wall from the left pulmonary venous antrum (segment 1). Antero-superiorly, the lateral wall is marked by the lateral border of the anterior wall and the appendage. The infero-posterior border is marked by the geodesic extending from point H, at the 4 o'clock position on the left atrioventricular junction, and point B marking the most inferior aspect of the left pulmonary venous antrum (*Figure 12*). If desired, sub-segments distinguishing the left lateral ridge (6a) from the remainder of the lateral wall (6b) may be defined.

The left lateral ridge (sub-segment 6a) represents the basal aspect of the lateral wall. Its superior border is defined by the shortest geodesic connecting point A, which marks the most superior aspect of the left antral boundary, and the orifice of the left appendage. The inferior border of the left lateral ridge is defined by the shortest geodesic connecting point B, or the most inferior aspect of the left antral boundary of segment 1 and the orifice of the appendage. The remainder of the lateral wall constitutes sub-segment 6b.

Segment 7: left atrial inferior wall (including sub-segments 7a, 7b, 7c, and 7d)

Anatomical, electrophysiological, and clinical considerations

The inferior wall, comprised of components belonging to the atrial body and vestibule, forms the wall, which extends along the cardiac axis from the dome to the hinge of the mural leaflet of the mitral valve. The vestibular component of the wall forms part of the boundary of the left inferior atrioventricular groove, within which is found the coronary sinus and, when dominant, the circumflex artery.

Definition of segmental boundaries

The cranial boundary of the inferior wall is defined by the inferior border of the dome, which is marked by the geodesic between points B and D. The apical boundary is the hinge line of the mural leaflet of the mitral valve in the left atrioventricular junction. The geodesic marking this boundary extends from point H, found at the 4 o'clock position, to point I at 7 o'clock. The lateral boundary with segment 6, and the septal boundary with segment 8, is marked by the geodesics connecting the points B and H, and D and I, respectively (*Figure 13*). The inferior

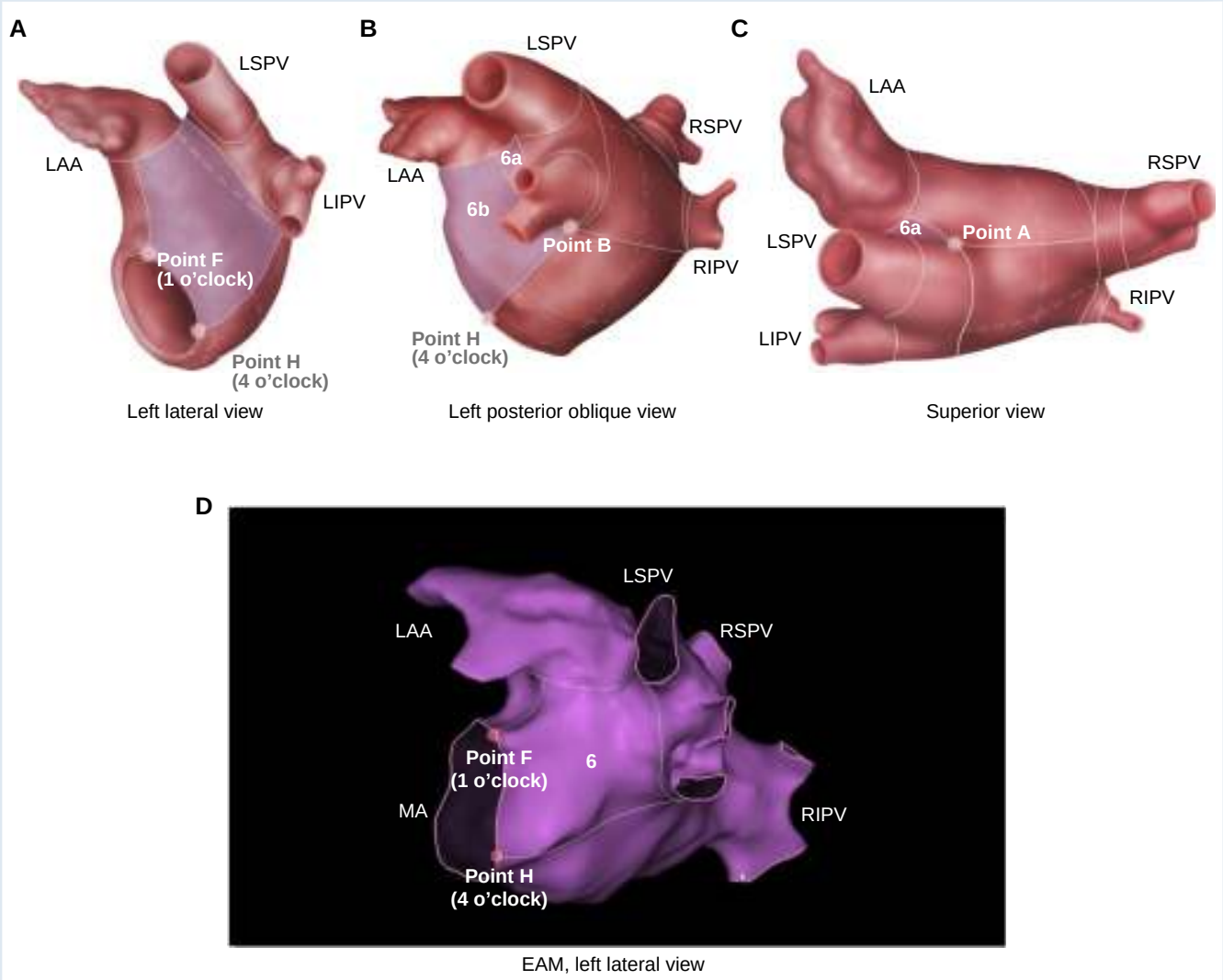

Figure 12 Segment 6 (left atrial lateral wall). Illustration of segment 6 in a left lateral view (*A*), a left posterior oblique view (*B*), and a superior view (*C*). (*D*) Clinical routine electroanatomical map visualizing segment 6 in a left lateral view. IVC, inferior vena cava; LAA, left atrial appendage; LSPV, left superior pulmonary vein; MA, mitral annulus (left atrioventricular junction) RSPV, right superior pulmonary vein; RIPV, right inferior pulmonary vein; SVC, superior vena cava.

wall can also be sub-divided into quadrants. A geodesic bisecting the septal and lateral borders of the inferior wall separates the basal from the apical quadrants. A second geodesic bisecting the first one can then be placed to separate the septal from the lateral quadrants.

Segment 8: left atrial septal wall

Anatomical, electrophysiological, and clinical considerations

The septal aspect of the left atrium, which makes up segment 8, is directly adjacent cranially to the right pulmonary venous antrum. Not all of this wall is septal. As we have explained, the true septum, which interposes between the cavities of the atrial chambers, is formed only by the floor of the oval fossa and its antero-inferior buttress.[33,34] When seen from the left side, the floor of the fossa overlaps its infolded rims, and has two characteristic horns. These are rarely visualized, when using clinical diagnostic modalities. The floor of the fossa, which forms the flap valve of the oval foramen, is the target for trans-septal puncture during catheter-based interventions. The wall selected to represent segment 8 also includes the infolded atrial walls that make up the superior, posterior, and inferior margins of the fossa.[33–35,37,58]

Definition of segmental boundaries

Apically, segment 8 is bordered by the margins of the left atrioventricular junction between point E, at the 9 o'clock position, and point I at 7 o'clock. The basal border is formed by the boundary with segment 2, or the right venous antrum. Antero-superiorly, the boundary is with the septal border of the anterior wall, or segment 4. This is marked by the geodesic extending between point E at 9 o'clock on the atrioventricular junction, and point C, which marks the intersection of the roof line with the right pulmonary venous antrum. The infero-posterior border is marked by the geodesic connecting point I, the 7 o'clock position on the junction, with point D, which marks the most inferior aspect of the right venous antrum (*Figure 14*).

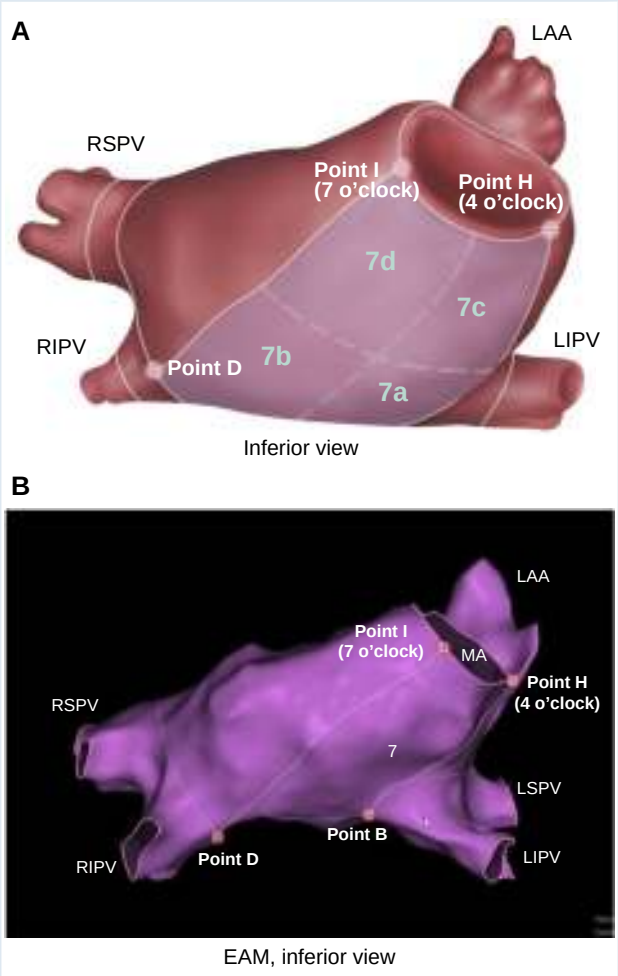

Figure 13 Segment 7 (left atrial inferior wall). Illustration of segment 7 in an inferior view (*A*) and a clinical routine electroanatomical map visualizing segment 7 in the same view (*B*). LAA, left atrial appendage; LIPV, left inferior pulmonary vein; LSPV, left superior pulmonary vein; MA, mitral annulus (left atrioventricular junction); RIPV, right inferior pulmonary vein; RSPV, right superior pulmonary vein.

Segmentation of the right atrium

Segment 9: right atrial septal wall

Anatomical, electrophysiological, and clinical considerations

As we have already discussed, the true atrial septum, which interposes between the atrial cavities, is formed only by the floor of the oval fossa and its antero-inferior buttress.[33,34] The septal aspect of the atrial cavity defined as segment 9, also includes all the paraseptal components of the atrial walls, except for the triangle of Koch. The paraseptal areas, found superiorly, posteriorly, and inferiorly are the infolded atrial walls, along with the fold between the orifices of the inferior caval vein and the coronary sinus known as the Eustachian ridge.[33–35,37,38,53,58]

Definition of segmental boundaries

The area defined as segment 9 extends from the right atrial posterior wall, which makes up segment 10, to the paraseptal region marked by the triangle of Koch, which is recognized as segment 15. The inferior border of segment 9 is defined by the geodesic connecting point J, marking the most inferior aspect of the orifice of the coronary sinus, with point K, marking the most septal aspect inferior caval vein orifice (*Figure 15*).

We should emphasize again that, when defining the borders of the right atrioventricular junction, we used the clock model, as was the case for the left atrioventricular junction (*Figure 2*). The co-ordinates of the model are themselves defined using the apico-basal view, which is parallel to the long cardiac axis and perpendicular to the tricuspid valvular plane. The superior boundary of segment 9 is then defined by the geodesic extending between point L, which marks the most septal aspect of the superior caval vein orifice, and point M, representing the superior septal aspect (1 o'clock position) of the right atrioventricular junction. The basal border is marked by the geodesic connecting points K and L, which represent the boundaries of the orifices of the caval veins closest to the septal surface. The apical boundary is formed by the orifice of the coronary sinus. It is defined by the geodesic between point M, at the superior septal aspect of the right atrioventricular junction, or the 1 o'clock position, and point J, which is placed at the most inferior aspect of the orifice of the coronary sinus.

Segment 10: right atrial posterior venous wall

Anatomical, electrophysiological, and clinical considerations

Segment 10 is formed by the walls of the systemic venous sinus, itself derived from the so-called sinus venosus.[29] In contrast to the pectinated walls of the adjacent appendage, the walls of the area between the orifices of the caval veins is characterized by its smooth endocardial surface.[53]

Endocardially, the border between the smooth venous component and the pectinated appendage is marked by the muscular ridge known as the terminal crest, or crista terminalis. Epicardially, the crest matches the location of the terminal groove, or sulcus terminalis. It may not be possible to identify these features using echocardiography, but they should now be recognized by those using computed tomography. As yet, however, we have not considered them to be identified with sufficient regularity to be used as region-defining landmarks in our model. The epicardial boundary between the appendage and the systemic venous sinus, nonetheless, is of significance because, in this area, the sinus node is found within the terminal groove. In most individuals the node lies inferior to the prominent crest of the appendage, which is also known as the arcuate ridge. In around one-tenth of individuals, the node can extend across the cavoatrial junction in horseshoe fashion. In all individuals, nonetheless, the node has a tail which extends caudally within the terminal groove towards the orifice of the inferior caval vein.[59] In addition to the location of the sinus node, the proximity of the phrenic nerve on the epicardial aspect of the systemic venous sinus has important implications for the ablation of atrial arrhythmias in this area.

Definition of segmental boundaries

Superiorly and inferiorly, the posterior venous wall is bounded by the orifices of the caval veins (*Figure 16*). The lateral border, formed by the terminal crest and the terminal groove, can also be marked by the geodesic connecting points N and O, which are placed on the most lateral aspects of the venous orifices. These points should be placed when using a basal-to-apical projection, a view that is parallel to the long cardiac axis. Using the same view, the septal border is marked by the geodesic placed between points K and L, which mark the most septal aspects of the venous orifices.

Segment 11: right atrial appendage and lateral wall (including sub-segments 11a and 11b)

Anatomical, electrophysiological, and clinical considerations

The right appendage has a characteristically triangular shape, with a particularly broad junction with the remainder of the atrial chamber. As such, it forms the entirety of the atrial wall of the right atrium when viewed externally (*Figure 17*). When assessed internally, however, the smooth vestibular component interposes throughout the parietal atrioventricular junction between the pectinated wall and the hinge of the

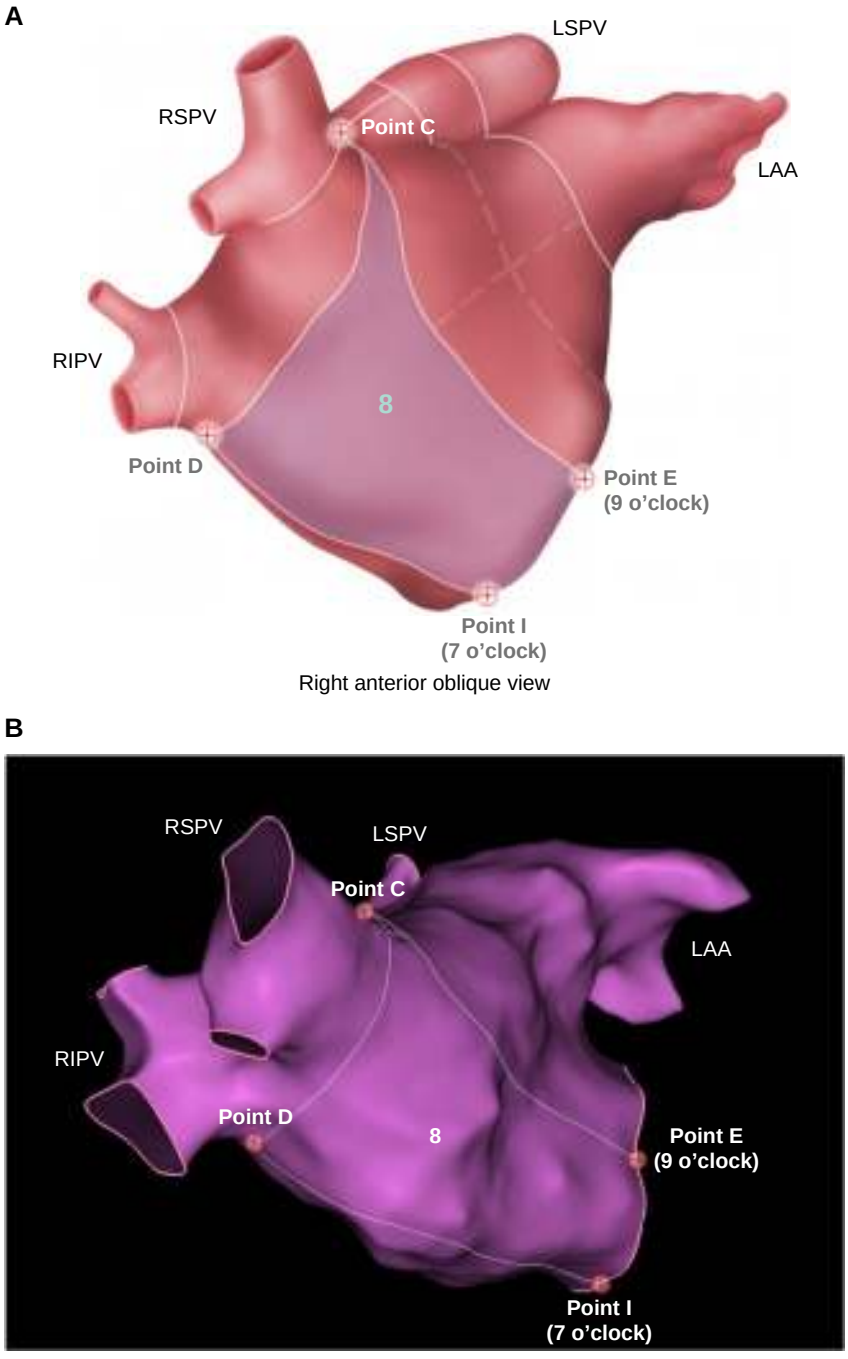

Figure 14 Segment 8 (left atrial septal wall). Illustration of segment 8 in a right anterior oblique view (*A*), and a clinical routine electroanatomical map visualizing segment 8 in the same view (*B*). LSPV, left superior pulmonary vein; LAA, left atrial appendage RIPV, right inferior pulmonary vein; RSPV, right superior pulmonary vein.

antero-superior and inferior leaflets of the tricuspid valve. Although the extent of the pectinated wall is obvious to the anatomist, these features currently remain more difficult to recognize in a reproducible, standardized manner using imaging or electroanatomical mapping modalities.[37,38,53,58]

The junction between the smooth venous component making up segment 10 and the pectinated wall of the appendage is formed by the terminal crest, which extends vertically from the antero-lateral aspect of the orifice of the superior caval vein towards the antero-lateral aspect of the inferior caval venous orifice. The crest has high relevance for electrophysiologists. The cardiomyocytes making up the crest are aggregated together in parallel fashion, thus producing one of the preferential pathways for conduction known to exist in the atrial walls. At the junction with the crest of the appendage, however, there is an area

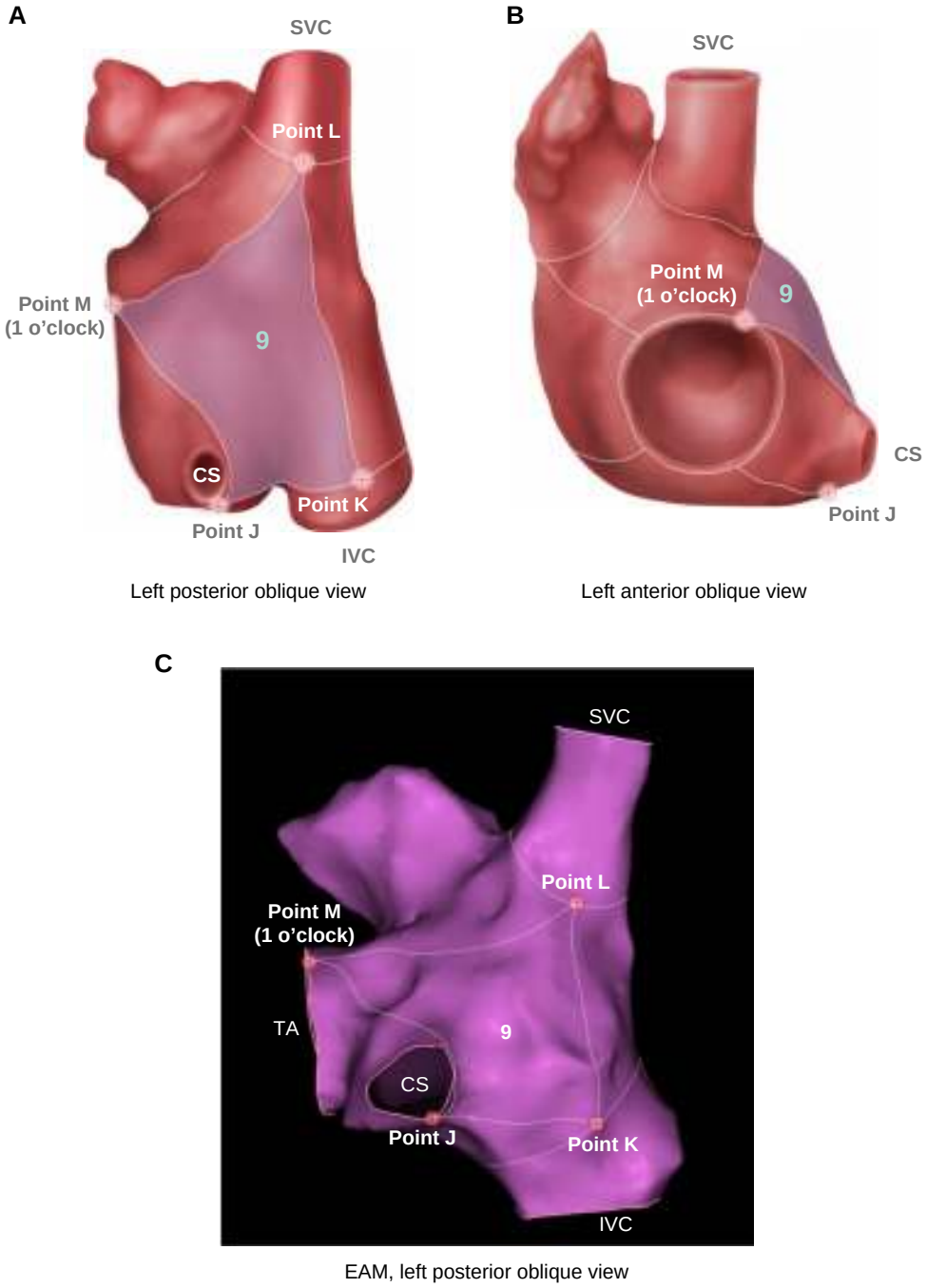

Figure 15 Segment 9 (right atrial septal wall). Illustration of segment 9 in a left posterior oblique view (*A*) and a left anterior oblique view (*B*). (*C*) Clinical routine electroanatomical map visualizing segment 9 in a left posterior oblique view. CS, coronary sinus; IVC, inferior vena cava; SVC, superior vena cava; TA, tricuspid annulus (right atrioventricular junction).

of non-uniform anisotropy, which is held to be arrhythmogenic.[35] Additional areas of arrhythmogenicity are also known to involve the length of the terminal crest, while the sinus node itself is found within the terminal groove.[37]

The pectinate muscles that characterize the endocardial surface of the appendage originate from the terminal crest. They extend in parallel fashion from the crest, reaching towards the vestibule throughout the parietal extent of the right atrioventricular junction. As is the case with the left appendage, the atrial wall between the individual pectinate muscles can be extremely thin, and is often described as 'parchment-like'.[38]

The appendage is usually used as the site for implantation of atrial pacemaker leads.[60]

Definition of segmental boundaries

From a strictly anatomical perspective, segment 11 in its entirety constitutes the atrial appendage. From an electrophysiological standpoint,

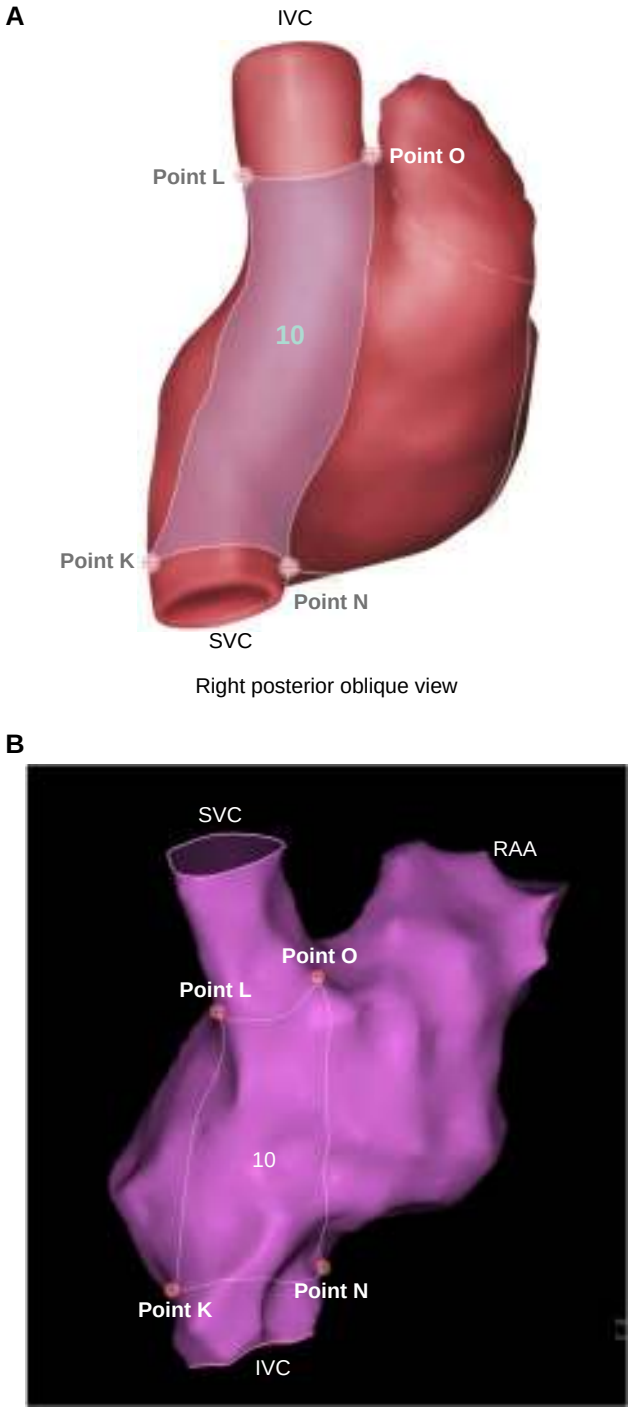

Figure 16 Segment 10 (right atrial posterior venous wall). Illustration of segment 10 in a right posterior oblique view (*A*) and a clinical routine electroanatomical map visualizing segment 10 in the same view (*B*). IVC, inferior vena cava; RAA, right atrial appendage; SVC, superior vena cava.

however, only the characteristic distal protrusion is commonly regarded as the atrial appendage. To resolve this discrepancy, we have defined corresponding sub-segments: sub-segment 11a, which describes the distal protrusion of the appendage, and sub-segment 11b, which corresponds to the lateral pectinate wall, that is likewise composed of appendage-defining pectinate muscle.

The anterior and superior borders of segment 11 can readily be appreciated and defined when using computed tomography or magnetic resonance imaging. The triangular antero-superior protrusion of the right atrial appendage is particularly characteristic, producing a pronounced anterior angulation with the remainder of the atrial cavity. Inferior to the protrusion, segment 11 shows a considerable

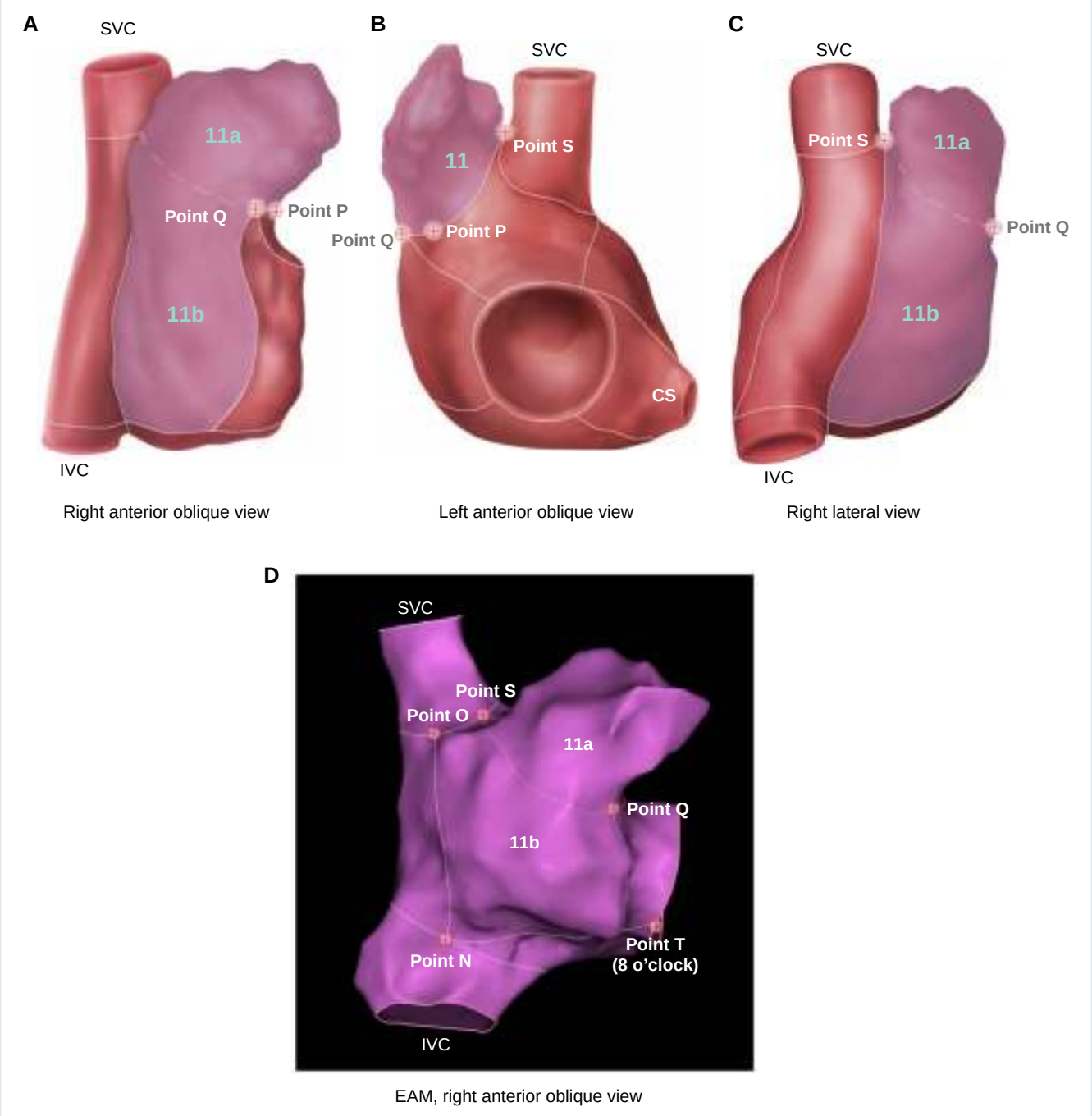

Figure 17 Segment 11 (right atrial appendage and lateral wall). Illustration of segment 11 in a right anterior oblique view (*A*), a left anterior oblique view (*B*), and a right lateral view (*C*). (*D*) Clinical routine electroanatomical map visualizing segment 11 in a right anterior oblique view. IVC, inferior vena cava; SVC, superior vena cava.

indentation as it transitions along the lateral wall towards the atrial vestibule, which is defined as segment 12 (see *Figure 17*).

Both aspects can be delineated directly, based on the maximum local concavity at these transitions. Not all imaging and mapping modalities, however, currently provide sufficient spatial resolution accurately to define these anatomical landmarks, particularly when using automatic algorithms. To facilitate standardized automated regionalization, therefore, we have established three auxiliary points to permit approximate recognition of the anterior and superior borders of segment 11.

Point P marks the anterior junction, at the site where the appendage protrudes from the remainder of the atrial cavity. This is the site of the prominent angulation. The point can thus be defined by the maximum concavity at the transition from the appendage to the anterior atrial wall.

Point Q marks the anterior junction of the protruding appendage with the lateral wall. It can be defined by the maximum anterior concavity of the lateral wall in a right lateral view. In individuals with a shift of the cardiac axis, the right lateral view may have to be adapted according

to the rotated cardiac axis, so that the angulation at the protruding appendage can be appreciated.

The final point, which is point S, marks the antero-superior cavoatrial junction. It is placed on the most anterior aspect of the superior caval venous orifice and should be determined using a right lateral view as well.

Having determined these three points, the border between the appendage and the anterior wall, or segment 13, is represented by a geodesic connecting these points anteriorly. Should the diagnostic modalities provide sufficient spatial resolution; the points can be connected simply by following the groove formed by the anterior angulation resulting from the protrusion of the distal part of the appendage. Automatic algorithms may determine this groove based on maximum local curvatures.

The inferior continuation of the border between the antero-lateral part of segment 11 and the lateral vestibule (segment 12) may be recognized as the anterior edge of the silhouette as seen in a right lateral view. Again, this view may have to be adapted according to the individual cardiac axis. Alternatively, should there be sufficient spatial resolution, the border can be delineated following the prominent ridge formed by the indentation of the lateral wall, based on maximum local curvatures. Inferiorly, this border intersects the cavotricuspid isthmus, which forms the inferior boundary of segment 11 (see segment 14 for details).

The posterior border of the appendage and the lateral wall is demarcated endocardially by the prominent terminal crest, with the epicardial border marked by the terminal groove. The appendage also stands out from the smooth posterior venous wall by virtue of its characteristic pectinate muscles. If the spatial resolution allows for identification of the terminal crest or groove, these can be used as landmarks marking the posterior border of the appendage. If neither the terminal groove nor the terminal crest can be identified, then a geodesic is created that connects the most lateral aspects of the caval venous orifices, with these representing points N and O as previously defined. Segment 11 can then be divided into a sub-segment 11a, corresponding to the protruding distal portion of the appendage, and an inferior subsegment 11b made up of the pectinate lateral wall. These sub-segments are defined by the geodesic connecting points Q and S posteriorly.

Segment 12: right atrial lateral vestibule

Anatomical, electrophysiological, and clinical considerations

The lateral vestibule is defined to produce segment 12, and forms part of the lateral wall. When assessed anatomically it includes part of the pectinated wall of the appendage, along with the lateral part of the vestibule. The atrial vestibule is made up by circumferentially aggregated cardiomyocytes that encircle the parietal part of the tricuspid valvular orifice. When assessed in gross specimens, the vestibule can readily be distinguished from the pectinated wall of the appendage by its smooth endocardial surface.[35]

Definition of segmental boundaries

The posterior junction between the vestibule and the appendage is indicated by a marked indentation, which is best appreciated in lateral or right anterior oblique view. In this view, images obtained with diagnostic modalities also show an abrupt caliber change at the transition between the vestibule and the appendage, that is, at the level of the vestibule, the right atrium has a significantly smaller diameter than more basally, at the level of the right atrial appendage. For the purposes of segmentation, we have included part of the appendage, together with the vestibule, to make up the lateral wall of the right atrium. The apical extent of this segment is the hinge of the antero-superior leaflet of the tricuspid valve. It extends inferiorly to reach the boundary with segment 14, which is dominated by the cavotricuspid isthmus. This inferior border can be marked by placing a geodesic between point T, which represents the infero-lateral aspect of the right atrioventricular junction, or 8 o'clock on the clock model, and the most lateral aspect of the inferior caval venous orifice, which has previously been defined as point N (*Figure 18*). The superior border of the lateral wall is marked by placing a geodesic from point U, which is at 11 o'clock relative to the right atrioventricular junction, to point Q placed at the anterior junction between the lateral wall and the wall defined to represent segment 11.

Segment 13: right atrial anterior wall

Anatomical, electrophysiological, and clinical considerations

Segment 13 is made up of all the components contributing to the anterior wall of the right atrial body. Hence, it includes the anterior part of the vestibule but excludes the anterior protrusion of the pectinated right appendage. Within the cranial and leftward part of this segment is found Bachmann's bundle. This part of the anterior interatrial groove, as was the case for the terminal crest, is characterized by the parallel aggregation of its contained working cardiomyocytes. The bundle commences at the pre-caval terminal crest, continues across the superior cavoatrial junction, and extends through the anterior wall of the left atrium towards the left lateral ridge.[35,37]

Also included in segment 13 is the superior paraseptal part of the atrial wall that joins the supraventricular crest of the right ventricle. This area is directly adjacent to the right coronary sinus of the aortic root.[31,61–64] This relationship, therefore, should be taken into account by those attempting trans-septal puncture, since too anterior a direction of the needle courts the risk of inadvertent aortic punctures. It is also reported that the parts of the wall inferior to Bachmann's bundle are exceptionally thin.[29]

Definition of segmental boundaries

As defined in the model, segment 13 extends basally from the superior aspects of the right atrioventricular junction towards the appendage and the superior cavoatrial junction. It is bordered laterally by the wall of segment 12. As with that segment, the anterior wall includes not only part of the vestibule, but also part of the appendage, although it may not always be possible clinically to identify the pectinated component. When traced superiorly, it reaches as far as the superior cavoatrial junction. Its septal border is marked by a geodesic drawn between point M, found at the 1 o'clock position in the right atrioventricular junction, and point L, which marks the most septal aspect of the superior cavoatrial junction (*Figure 19*).

Segment 14: cavotricuspid isthmus

Anatomical, electrophysiological, and clinical considerations

This segment, as defined for the purpose of the model, has three parts. The central part, which is also the most inferior part, represents the cavotricuspid isthmus as defined anatomically. The second part is a paraseptal area producing the most inferior aspect of the inferior pyramidal space at the base of the triangle of Koch. The third part forms an infero-lateral area that again includes part of the anatomical vestibule.[37]

It is well-established that typical atrial flutter is effectively abolished when an ablation line is created extending from the right atrioventricular junction to the inferior cavoatrial junction, with the shortest distance between the two isolating anatomical structures being at the level of the anatomically defined isthmus. Unlike the paraseptal area, this inferior isthmus is usually devoid of critical structures at risk for collateral damage, such as the right coronary artery, the atrioventricular node, or the artery to the node. The anatomical isthmus, furthermore, usually possesses the thinnest walls, thus facilitating trans-mural ablation in this area when compared to the rather thicker walls of the infero-lateral component of the segment. Of note, catheter ablation is often complicated by presence of a particularly prominent Eustachian valve.[35] The origin of the Eustachian valve from the inferior part of the Eustachian ridge marks the posterior boundary of the isthmus as defined anatomically. Within the anatomical isthmus, the presence of the deep sub-Thebesian recess may further impede effective catheter ablation.[35,37]

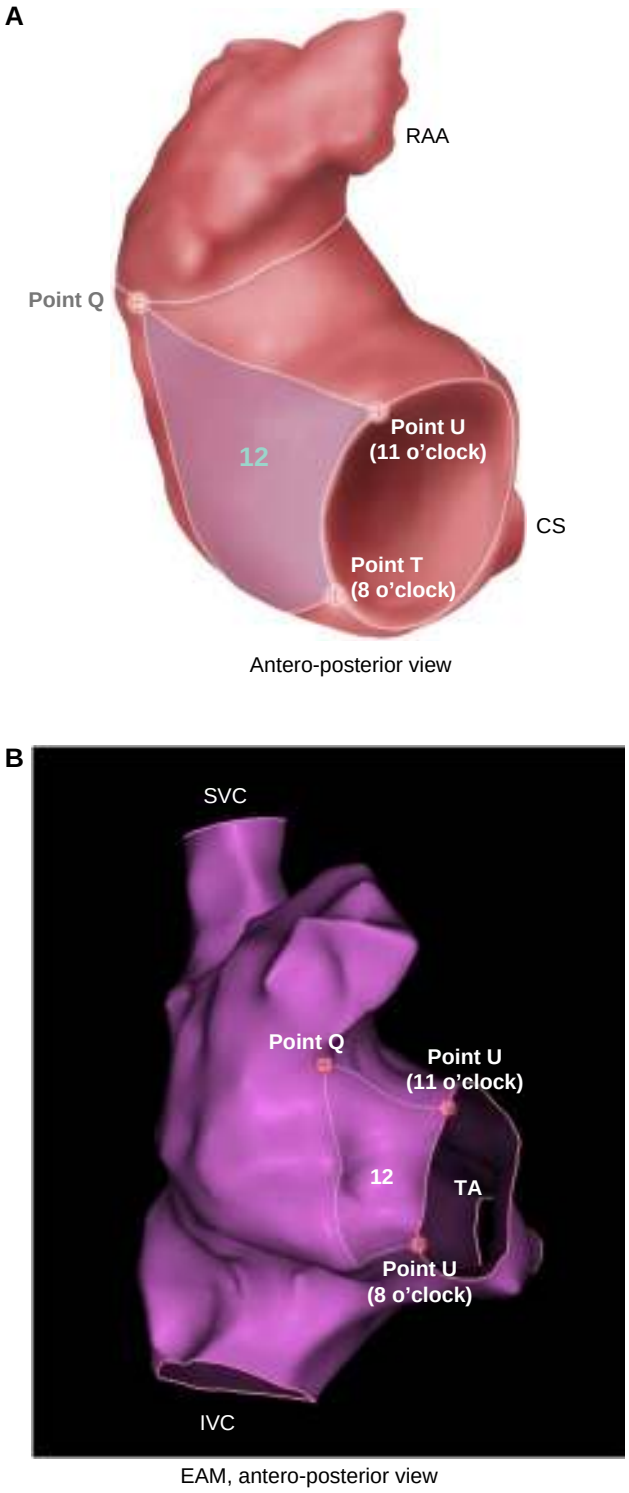

Figure 18 Segment 12 (right atrial lateral vestibule). Illustration of segment 12 in an antero-posterior view (*A*) and a clinical routine electroanatomical map visualizing segment 12 in the same view (*B*). IVC, inferior vena cava; SVC, superior vena cava; TA, tricuspid annulus (right atrioventricular junction).

Definition of boundaries for 3D imaging and electroanatomical mapping

The area defined as representing segment 14 extends from the inferior cavoatrial junction to the hinge line of the inferior leaflet of the tricuspid valve in the right atrioventricular junction (*Figure 20*). On the septal side, it is bounded by segment 9 and by the floor of the triangle of Koch, with the latter defined as representing segment 15. Accordingly, the septal border can be defined by creating geodesics, which connect point J, marking the inferior border of the orifice of the coronary sinus, with

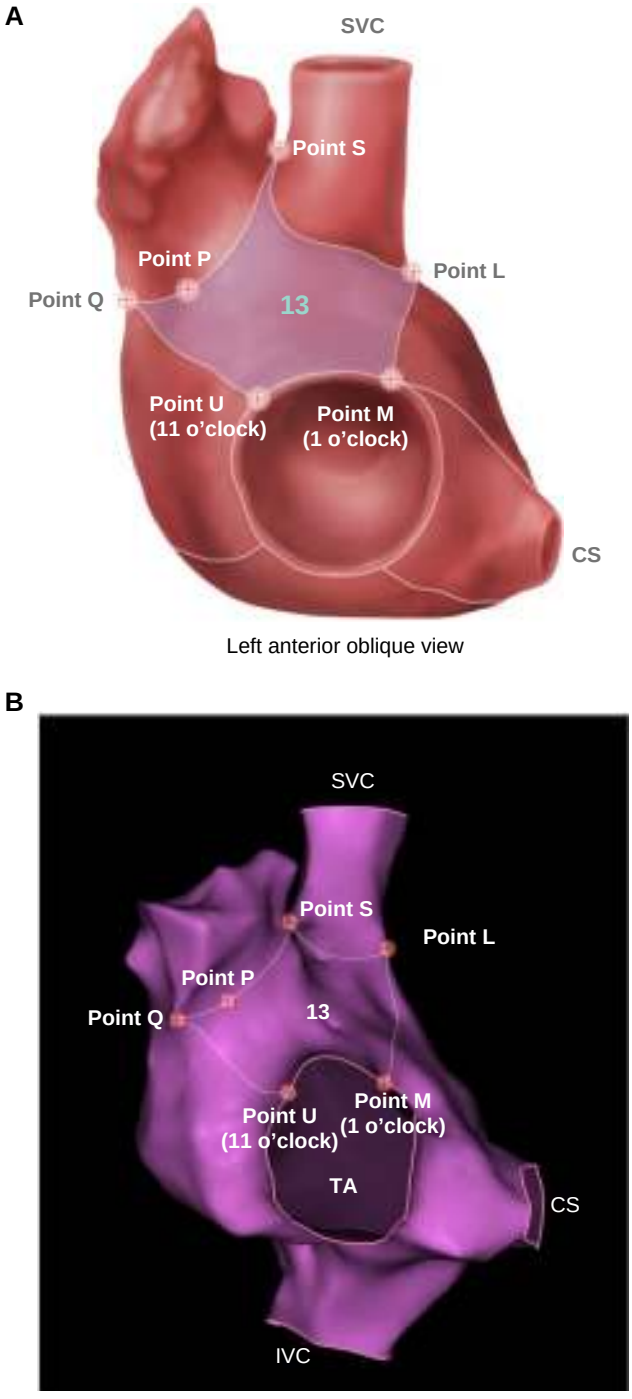

Figure 19 Segment 13 (right atrial anterior wall). Illustration of segment 13 in a left anterior oblique view (*A*) and a clinical routine electroanatomical map visualizing segment 13 in the same view (*B*). CS, coronary sinus; IVC, inferior vena cava; SVC, superior vena cava; TA, tricuspid annulus (right atrioventricular junction).

point K, placed at the most septal aspect of the inferior cavoatrial junction, and with point V, placed at 5 o'clock within the right atrioventricular junction. The lateral boundary is then determined by the geodesic connecting point T, the 8 o'clock position in the right atrioventricular junction, with point N, previously defined as the most lateral aspect of the inferior cavoatrial junction.

Segment 15: Koch's triangle

Anatomical, electrophysiological, and clinical considerations

Segment 15 is the right atrial wall of the pyramid of Koch. This important area harbours such crucial electrophysiologically and clinically relevant structures as the compact atrioventricular node, the site of penetration of the atrioventricular conduction axis, and the

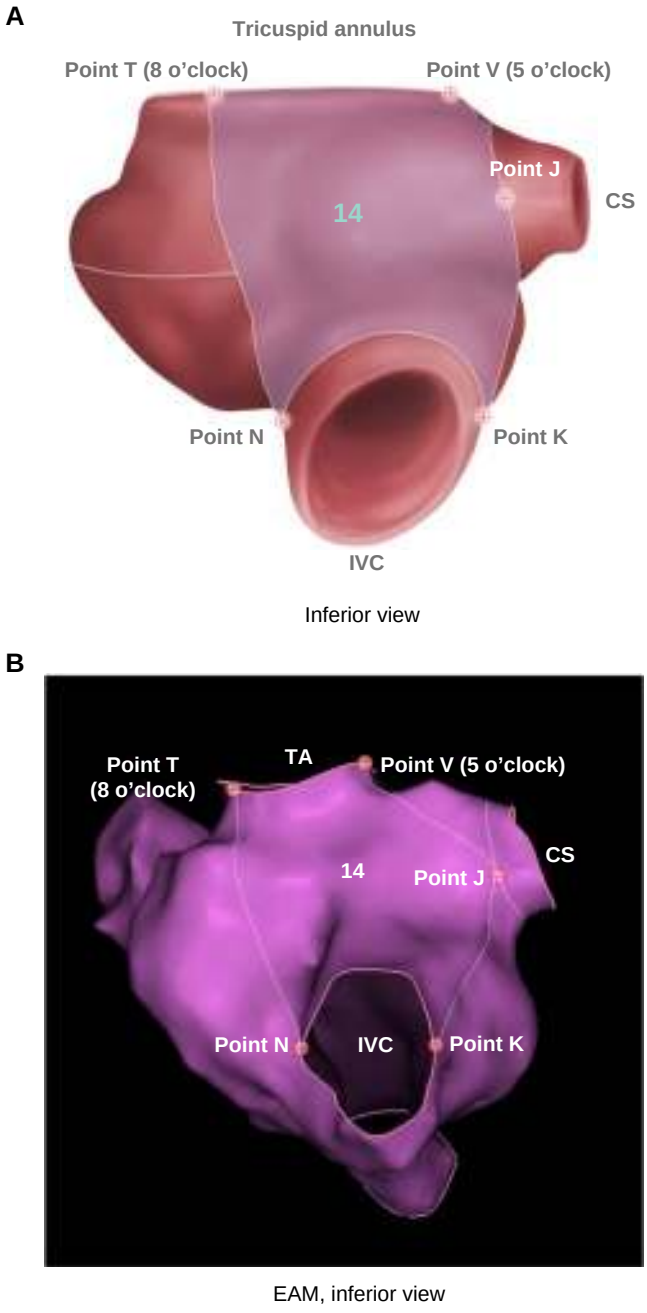

Figure 20 Segment 14 (cavotricuspid isthmus). Illustration of segment 14 in an inferior view (*A*), and a clinical routine electroanatomical map visualizing segment 14 in the same view (*B*). CS, coronary sinus; IVC, inferior vena cava; TA, tricuspid annulus (right atrioventricular junction).

slow pathway into the node. The conduction axis penetrates to become the non-branching atrioventricular bundle at the apex of the pyramid, with this region often described as being para-Hisian area.[31,61–64] The area is a common origin of focal atrial tachycardias. It is also a typical location for the atrial insertions of paraseptal or septal accessory pathways, these pathways also often described as being para-Hisian. The triangle of Koch itself serves as a reference for anatomically guided catheter ablation of the slow nodal pathway in treatment of atrioventricular nodal re-entrant tachycardias.[35,37]

The apical border of the triangle is the hinge of the septal leaflet of the tricuspid valve. The two sides of the triangle come together at the site of the part of the central fibrous body formed by the atrioventricular component of the membranous septum. It is in this area where the conduction axis becomes insulated from the atrial myocardium to become the non-branching bundle. The last atrial cardiomyocytes that join with the axis prior to its insulation are also found in the apex of the triangle, forming the fast pathway into the node. The base of the triangle is formed by the coronary sinus and by the atrial vestibule between the anterior margin of the coronary sinus and the hinge of the septal leaflet

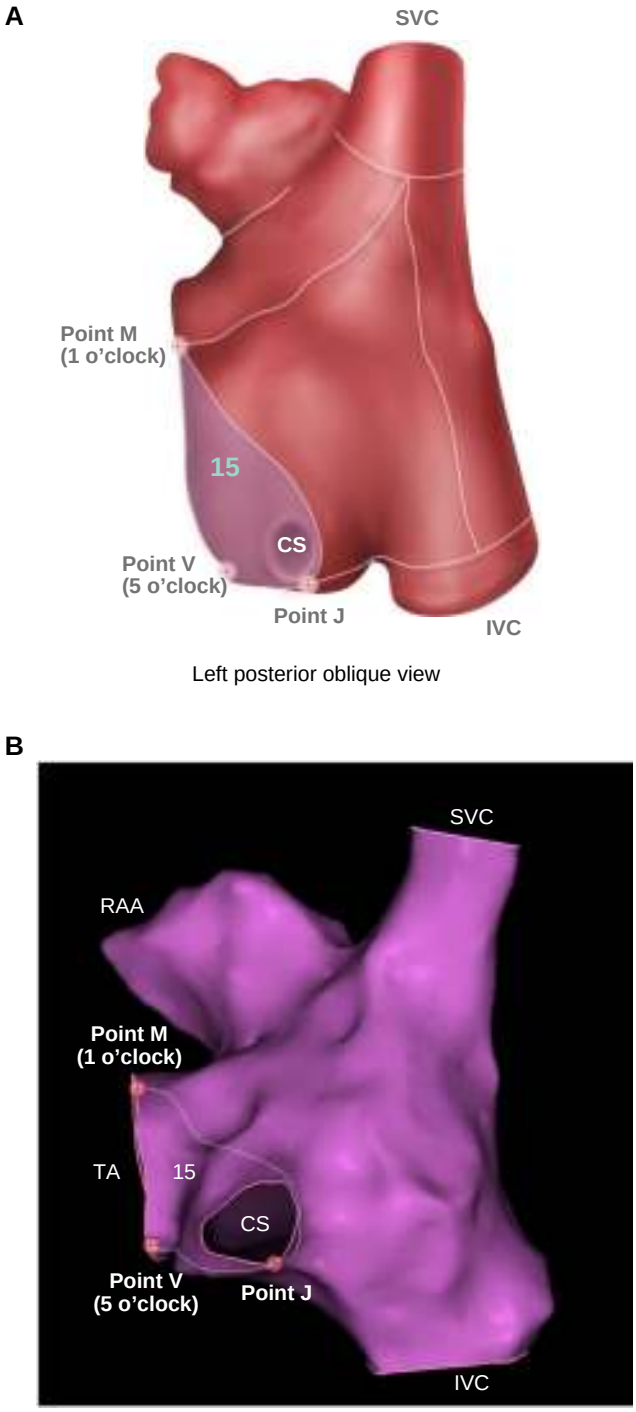

Figure 21 Segment 15 (Koch's triangle). Illustration of segment 15 in a left posterior oblique view (*A*), and a clinical routine electroanatomical map visualizing segment 15 in the same view (*B*). CS, coronary sinus; IVC, inferior vena cava; RAA, right atrial appendage; SVC, superior vena cava; TA, tricuspid annulus (right atrioventricular junction).

of the tricuspid valve. This second area forms an obvious paraseptal isthmus. It is in this region where the slow pathway is typically targeted during catheter ablation of atrioventricular nodal re-entrant tachycardias.[35,37]

The superior area at the apex of the triangle is directly adjacent to the right coronary sinus of the aortic root.[31,61–64] This relationship should be taken into account during trans-septal puncture, where too anterior a direction of the needle may result in inadvertent aortic puncture.

Definition of segmental boundaries

The apical border of the triangle is marked by the hinge of the septal leaflet of the tricuspid valve at the right atrioventricular junction. It is defined by points M and V, found at 1 o'clock and 5 o'clock when using the clock model (*Figure 21*). The triangle is bordered inferiorly by segment 14, with the border being defined by the geodesic connecting the point V in the infero-septal aspect of the right atrioventricular junction and point J, marking the inferior part of the mouth of the coronary sinus. Towards the interatrial septum, the triangle is bordered by the geodesic between point M in the right atrioventricular junction and point J at the inferior border of the mouth of the coronary sinus. This geodesic passes posterior to the mouth of the sinus.

Discussion

Our multi-disciplinary consensus presents a standardized bi-atrial regionalization based on anatomical, electrophysiological, and clinical considerations that can universally be applied to 3D atrial geometries derived from imaging, electroanatomical mapping or computational modelling. Three-dimensional imaging and high-resolution electroanatomical mapping have now become an integral part of cardiac electrophysiology and the management of patients with arrhythmias.[65–67] With further technological advances the significance of these modalities continues to grow.

Clinical and scientific impact

Regional approaches may improve our understanding of atrial cardiomyopathies and the associated risk of arrhythmias and stroke.[1] It is now well-established that the regional distribution of atrial arrhythmogenic substrates, rather than their mere presence or extent, is a key determinant of the risk of arrhythmias and their underlying mechanisms. This has been shown for various surrogates of arrhythmogenic substrate in imaging, such as late gadolinium enhancement in cardiac resonance imaging, electroanatomical mapping of areas of local low-voltage or slow conduction, and computational modelling studies.[13,15,43,68]

Moreover, combining imaging- and artificial intelligence-based methods, regional morphological features and tissue composition, have been linked to the risk of stroke.[69] It is now the case that 3D imaging and mapping technologies allow for the accurate localization of both arrhythmogenic and thrombogenic substrates.[52,70–72] A universal definition is required of the atrial regions and their boundaries, nonetheless, if we are to perform regional quantitative analyses, and to make intra- and inter-individual, as well as cross-modality comparisons.

Finally, regional assessment of the atria may help to guide personalized therapies for atrial fibrillation. Based on the spatial distribution of the individual arrhythmogenic substrate, treatment decisions may be substantiated and targeted regional ablation approaches may be developed.[15,17] Again, to test and establish such personalized therapies, standardization in terms of well-defined, reproducible target regions will be essential.

15-Segment bi-atrial model

Already in 2002, a scientific statement made on behalf of the American Heart Association proposed a standardized regionalization of the left ventricle based on a 17-segment model. This model for the left ventricle is widely accepted and routinely used.[12] There is no comparable standardized regionalization of the atrial chambers. Our 15-segment bi-atrial model as presented here, therefore, as far as we are aware, constitutes the first attempt to provide a comparable standardized regionalization for the atriums. Our proposed model, furthermore, conforms to all the criterions forming the basis of the scientific statement on standardized segmentation as established by the American Heart Association. In the first place, it maintains consistency with accepted anatomic and autopsy data. Second, it uses as much as possible the existing and accepted approaches to myocardial segmentation and nomenclature. Thirdly, whenever possible it provides precise localization by using anatomical landmarks. Finally, it permits adequate sampling without exceeding the limits of resolution of the imaging modalities or breaching the relevance for clinical and research applications.

Previous atrial regionalizations

Numerous studies have defined atrial components, either to guide catheter ablation, to study systematically local electrophysiological, functional or structural properties, or to establish the regional distribution of arrhythmogenic substrates.[13–15,43,49,50] The regionalization in these studies, however, did not aim at universal applicability. Instead, the regions were established to accommodate the specific demands of the respective study. Any regional definition published to date, therefore, is based on the inherent strengths and limitations of the applied imaging technique and the specific research objective, rather than on general anatomical, functional, or electrophysiological considerations.

As an example, in their study using cardiac magnetic resonance to establish the regional distribution of late gadolinium enhancement as a surrogate for arrhythmogenic substrate, one group defined 12 segments in the left atrium.[50] Because of their specific objectives and methodology, they excluded the entirety of the right atrium and the left appendage from their regionalization. They also failed to consider the pulmonary venous antrums as distinct segments, despite their known electrophysiological properties and clinical relevance. Similarly, in a recent multi-centric randomized clinical trial, Huo and associates did not consider the left appendage and the right atrium when defining atrial regions to determine the regional distribution of low-voltage areas to be targeted by catheter ablation.[15] In fact, the majority of regional analyses, and the corresponding segmental models developed, have focused only on the left atrium.

All atrial regionalizations of which we are aware to have been published to date have in common a lack of precision for definition of the proposed regions. Because of this, they do not allow for a reproducible delineation of atrial regions and their borders. This limitation also applies to the few bi-atrial regional analyses that have been conducted. While basically considering all relevant regions in the left and right atrium for their analyses of local complex fractionated atrial electrograms, three studies did not specify the exact borders of the regions they were investigating.[17–19] The bi-atrial regionalization proposed by Haissaguerre *et al.* constitutes an example in this respect.[14] Their regional analyses of the local drivers of atrial fibrillation determined by non-invasive electroanatomical mapping is based on a division of the atriums into no more than seven segments. This rough division, which fails to distinguish relevant structures such as the pulmonary venous antrums or the left appendage, may accommodate the limited spatial resolution of their chosen diagnostic modality. It is inappropriate for higher resolution modalities such as cardiac computed tomography or endocardial multi-electrode mapping. Hence, it lacks universal application. It also fails to detail the exact borders of the atrial regions as defined, thus rendering impossible reproducible regional definition.

In contrast to these previous attempts, when creating our 15-segment bi-atrial model, we defined our chosen segments using well-established anatomical, electrophysiological, and clinical considerations. The regional borders were clearly defined so as to enable reproducible regionalization. While the segmental borders have been determined with precision, the model can be readily adapted according to individual demands. For example, depending on the objective of a given study, or the spatial resolution of an underlying method, prespecified sub-divisions can be added, or different segments can be combined while maintaining standardized borders.

Standardized nomenclature and axes

Owing to the current limitations and the variable resolution of underlying imaging or mapping modalities, along with the relative absence of

detectable landmarks, we did not consider it appropriate to define the segments according to anatomical or morphological features. Hence, the use of standardized axes and planes, as well as an understandable terminology, are pre-requisites for reproducible regionalization. The nomenclature we have used complies with the so-called attitudinally appropriate approach. It uses trans-axial orthogonal projections defined according to the subject standing upright in the so-called anatomical position. This nomenclature was first proposed as early as 1975, and has gradually been accepted as a general standard.[24–27] Wherever it was more appropriate, nonetheless, we also used the cardiac long axis when defining the bi-atrial model, as proposed in the scientific statement from the American Heart Association on standardized cardiac segmentation and nomenclature for tomographic imaging of the heart.[12] In this respect, the cardiac long axis is usually well aligned with the plane of the atrial septum. It is ideally suited, therefore, to define septal as opposed to lateral, and basal vs. apical, directions in the atriums.[29]

Based on these standard axes, and their corresponding projections, when anatomical landmarks are lacking, or the spatial resolution of the underlying modality does not allow for their detection, we have created auxiliary points and planes to provide reproducible definitions of regional boundaries. The construction of regional borders based on these auxiliary points and planes might appear somewhat arbitrary. These borders, furthermore, are not always fully congruent with the anatomical and morphological boundaries. The creation of the auxiliary points and planes, however, favours reproducibility. Their optional application allows for accommodation of different degrees of spatial resolution depending on the underlying modality. It remains a fact that, wherever well-detectable anatomical landmarks or morphological features are lacking in the context of limited spatial resolution, an inevitable trade-off must remain between anatomical accuracy on the one hand, and standardization on the other hand.

Automatic regionalization

Our primary objective when creating our 15-segment bi-atrial model was to define regional borders with sufficient precision for them to be delineated in imaging-derived geometries in a reproducible and investigator-independent manner. As a proof-of-concept, the accomplishment of this objective was confirmed by the application of two independent software algorithms. We found that, when using datasets prepared with computed tomography or magnetic resonance imaging to establish atrial geometries from a group of 100 patients, the regional borders automatically delineated by those algorithms displayed very good agreement with our proposed regional definitions, thus demonstrating the reproducibility and universal applicability of the 15-segment bi-atrial model.[22,23] Thus, we could show that our atrial regionalization is widely applicable and well reproducible. While the automatic algorithms were developed for CT- and MRI images, the bi-atrial model is readily applicable also to modalities like 3D-echocardiography and computational modelling of sufficient quality.[73]

It is noteworthy, however, that the bi-atrial regionalization model was not specifically designed for the broad spectrum of congenital heart disease, and it remains to be determined to what extent our proposed model is applicable in this context. While the general concepts of the model should apply universally, specific adaptations of the border definitions may be required depending on the underlying entity. This is, however, beyond the scope of this document.

Conclusion

We have presented a standardized regionalization of the cardiac atriums for 3D imaging, electroanatomical mapping, and computational modelling as based on anatomical, electrophysiological and clinical considerations. The reproducibility and universal applicability of the 15-segment bi-atrial model was validated by use of two software algorithms independently developed for automatic regionalization. Our model, developed by consensus with a large group of experts, will ideally enable consistent regional analyses and homogeneous data acquisition across different centres and modalities. It will thus facilitate the employment of digital health- and artificial intelligence-based approaches. In this way, we anticipate our model will have a significant impact on arrhythmia research and on personalized approaches for the prevention and treatment of arrhythmias.

Acknowledgements

The authors thank the EHRA Scientific Document Committee: Katja Zeppenfeld (Chairperson), Jens Cosedis Nielsen (Co-Chairperson), Maria Frausing, Estelle Gandjbakhch, Isabelle C. van Gelder, Georgios Kollias, Michael Kühne, Radoslaw Lenarczyk, Petr Peichl, Archana Rao, Avi Sabbag, Frederic Sacher, Michelle Samuel, and Hadrian Wijnmaalen.

Funding

This project has received funding from the European Union's Horizon Europe Framework Programme under the Marie Skłodowska-Curie grant agreement No. 860974 (disclaimer: this publication reflects only the authors' view and the agency is not responsible for any use that may be made of the information it contains).

Conflict of interest: None of the authors have a conflict of interest related to this work. T.F.A. has received research grants for investigator-initiated trials from Biosense Webster and honoraria as a lecturer and consultant for ABBOTT Medical Devices and Corify Care. S.E.P. provides consultancy to Circle Cardiovascular Imaging, Inc., Calgary, Alberta, Canada. R.N. declares unrestricted research grants from Biotronik and Philips Volcano. C.S. declares an industrial cooperation with Medtronic. U.S. received consultancy fees or honoraria from Università della Svizzera Italiana (USI, Switzerland), Roche Diagnostics (Switzerland), EP Solutions Inc. (Switzerland), Johnson & Johnson Medical Limited, (UK), Bayer Healthcare (Germany). U.S. is co-founder and shareholder of YourRhythmics BV, a spin-off company of the University Maastricht. A.M.C. and M.S.G. are co-founders of Corify Care and receive honoraria from the company.

Data availability

The data underlying this article will be shared upon reasonable request to the corresponding author.

References

1. Goette A, Corradi D, Dobrev D, Aguinaga L, Cabrera JA, Chugh SS *et al.* Atrial cardiomyopathy revisited-evolution of a concept: a clinical consensus statement of the European Heart Rhythm Association (EHRA) of the ESC, the Heart Rhythm Society (HRS), the Asian Pacific Heart Rhythm Society (APHRS), and the Latin American Heart Rhythm Society (LAHRS). *Europace* 2024;**26**:euae204.
2. Van Gelder IC, Rienstra M, Bunting KV, Casado-Arroyo R, Caso V, Crijns H *et al.* 2024 ESC guidelines for the management of atrial fibrillation developed in collaboration with the European Association for Cardio-Thoracic Surgery (EACTS). *Eur Heart J* 2024;**45**:3314–414.
3. Donal E, Lip GY, Galderisi M, Goette A, Shah D, Marwan M *et al.* EACVI/EHRA Expert Consensus Document on the role of multi-modality imaging for the evaluation of patients with atrial fibrillation. *Eur Heart J Cardiovasc Imaging* 2016;**17**:355–83.
4. de Groot NMS, Shah D, Boyle PM, Anter E, Clifford GD, Deisenhofer I *et al.* Critical appraisal of technologies to assess electrical activity during atrial fibrillation: a position paper from the European Heart Rhythm Association and European Society of Cardiology Working Group on eCardiology in collaboration with the Heart Rhythm Society, Asia Pacific Heart Rhythm Society, Latin American Heart Rhythm Society and Computing in Cardiology. *Europace* 2022;**24**:313–30.
5. Althoff TF, Porta-Sanchez A. Does the spatial distribution of atrial arrhythmogenic substrate matter? Insights from the DECAAF II trial. *Europace* 2023;**25**:euad282.
6. Hopman LHGA, Bhagirath P, Mulder MJ, Eggink IN, van Rossum AC, Allaart CP *et al.* Quantification of left atrial fibrosis by 3D late gadolinium-enhanced cardiac magnetic resonance imaging in patients with atrial fibrillation: impact of different analysis methods. *Eur Heart J Cardiovasc Imaging* 2021;**23**:1182–90.
7. Alderete J, Fernández-Armenta J, Zucchelli G, Sommer P, Nazarian S, Falasconi G *et al.* The Ablate-by-LAWT multicentre prospective study: personalized paroxysmal atrial

fibrillation ablation with ablation index adapted to local left atrial wall thickness. *J Interv Card Electrophysiol* 2024;**67**:2089–99.
8. Mont L, Roca-Luque I, Althoff TF. Ablation lesion assessment with MRI. *Arrhythm Electrophysiol Rev* 2022;**11**:e02.
9. Nairn D, Eichenlaub M, Müller-Edenborn B, Huang T, Lehrmann H, Nagel C *et al.* Differences in atrial substrate localization using late gadolinium enhancement-magnetic resonance imaging, electrogram voltage, and conduction velocity: a cohort study using a consistent anatomical reference frame in patients with persistent atrial fibrillation. *Europace* 2023;**25**:euad278.
10. Regany-Closa M, Pomes J, Arbelo E, Guichard JB, Porta-Sanchez A, Guasch E *et al.* Postablation arrhythmogenic channels predict atrial fibrillation recurrence: iatrogenic substrate revisited. *JACC Clin Electrophysiol* 2025;**11**:823–6.
11. Lüscher TF, Wenzl FA, D'Ascenzo F, Friedman PA, Antoniades C. Artificial intelligence in cardiovascular medicine: clinical applications. *Eur Heart J* 2024;**45**:4291–304.
12. Cerqueira MD, Weissman NJ, Dilsizian V, Jacobs AK, Kaul S, Laskey WK *et al.* Standardized myocardial segmentation and nomenclature for tomographic imaging of the heart. A statement for healthcare professionals from the Cardiac Imaging Committee of the Council on Clinical Cardiology of the American Heart Association. *Circulation* 2002;**105**:539–42.
13. Assaf A, Mekhael M, Noujaim C, Chouman N, Younes H, Feng H *et al.* Effect of fibrosis regionality on atrial fibrillation recurrence: insights from DECAAF II. *Europace* 2023;**25**: euad199.
14. Haissaguerre M, Hocini M, Denis A, Shah AJ, Komatsu Y, Yamashita S *et al.* Driver domains in persistent atrial fibrillation. *Circulation* 2014;**130**:530–8.
15. Huo Y, Gaspar T, Schönbauer R, Wójcik M, Fiedler L, Roithinger FX *et al.* Low-voltage myocardium-guided ablation trial of persistent atrial fibrillation. *NEJM Evid* 2022;**1**: EVIDoa2200141.
16. Padilla-Cueto D, Ferro E, Garre P, Prat S, Guichard JB, Perea RJ *et al.* Non-invasive assessment of pulmonary vein isolation durability using late gadolinium enhancement magnetic resonance imaging. *Europace* 2023;**25**:360–5.
17. Invers-Rubio E, Hernández-Romero I, Reventos-Presmanes J, Ferro E, Guichard JB, Regany-Closa M *et al.* Regional conduction velocities determined by noninvasive mapping are associated with arrhythmia-free survival after atrial fibrillation ablation. *Heart Rhythm* 2024;**21**:1570–80.
18. Starreveld R, van der Does L, de Groot NMS. Anatomical hotspots of fractionated electrograms in the left and right atrium: do they exist? *Europace* 2019;**21**:60–72.
19. Chen YL, Ban JE, Park YM, Choi JI, Park SW, Kim YH. The spatial distribution of atrial fibrillation termination sites in the right atrium during complex fractionated atrial electrograms-guided ablation in patients with persistent atrial fibrillation. *J Cardiovasc Electrophysiol* 2013;**24**:949–57.
20. ESC Scientific Document Policy. European Society of Cardiology 2023. https://www.escardio.org/staticfile/Escardio/About%20the%20ESC/Documents/ESC-Scientific-Document-Policy.pdf (12 July 2025, date last accessed).
21. ESC Clinical Practice Guidelines: Policies and Procedures. European Society of Cardiology 2022. https://www.escardio.org/static-file/Escardio/Guidelines/Documents/2024%20Documents/ESC%20Clinical%20Practice%20Guidelines%20-%20Policies%20and%20Procedures.pdf (12 July 2025, date last accessed).
22. Althoff TF, Goetz C, Martinez LP, Invers-Rubio E, Hussain S, Mont L *et al.* Standardized regionalization of the atria for 3D cardiac imaging, electroanatomical mapping and computational modeling. A multidisciplinary consensus of the PersonalizeAF consortium. *Europace* 2024;**26**:euae102.064.
23. Goetz C, Martinez LM, Invers-Rubio E, Hussain S, Mont L, Schmidt C *et al.* PO-02-078 standardized regionalization of the atria for 3D cardiac imaging, electroanatomical mapping and computational modeling—a multidisciplinary consensus of the PersonalizeAF consortium. *Heart Rhythm* 2024;**21**:S292.
24. Cook AC, Anderson RH. Attitudinally correct nomenclature. *Heart* 2002;**87**:503–6.
25. Cosío FG, Anderson RH, Becker A, Borggrefe M, Campbell RW, Gaita F *et al.* Living anatomy of the atrioventricular junctions. A guide to electrophysiological mapping. A Consensus Statement from the Cardiac Nomenclature Study Group, Working Group of Arrythmias, European Society of Cardiology, and the Task Force on Cardiac Nomenclature from NASPE. North American Society of Pacing and Electrophysiology. *Eur Heart J* 1999;**20**:1068–75.
26. McAlpine WA. *Heart and Coronary Arteries: An Anatomical Atlas for Clinical Diagnosis, Radiological Investigation, and Surgical Treatment*. Heidelberg, Germany: Springer-Verlag; 1975.
27. Farré J, Anderson RH, Cabrera JA, Sánchez-Quintana D, Rubio JM, Benezet-Mazuecos J *et al.* Cardiac anatomy for the interventional arrhythmologist: I.terminology and fluoroscopic projections. *Pacing Clin Electrophysiol* 2010;**33**:497–507.
28. Anderson RH, Back Sternick E, Mahmud R, Cabrera JA, Katritsis D, Farre J *et al.* How best to describe the location of the substrates for abnormal cardiac rhythms. *Heart Rhythm* 2024;**21**:2377–85.
29. Mori S, Shivkumar K. *Atlas of Cardiac Anatomy*. Hopkins, USA: Cardiotext Publishing; 2022.
30. Hikspoors J, Kruepunga N, Mommen GMC, Köhler SE, Anderson RH, Lamers WH. A pictorial account of the human embryonic heart between 3.5 and 8 weeks of development. *Commun Biol* 2022;**5**:226.
31. Tretter JT, Spicer DE, Sánchez-Quintana D, Back Sternick E, Farré J, Anderson RH. Miniseries 1-Part III: 'Behind the scenes' in the triangle of Koch. *Europace* 2022;**24**: 455–63.
32. Cabrera JA, Sánchez-Quintana D, Farré J, Rubio JM, Ho SY. The inferior right atrial isthmus: further architectural insights for current and coming ablation technologies. *J Cardiovasc Electrophysiol* 2005;**16**:402–8.
33. Barbero U, Ho SY. Anatomy of the atria: a road map to the left atrial appendage. *Herzschrittmacherther Elektrophysiol* 2017;**28**:347–54.
34. Ho SY, Cabrera JA, Sanchez-Quintana D. Left atrial anatomy revisited. *Circ Arrhythm Electrophysiol* 2012;**5**:220–8.
35. Soto N, Datino T, Gonzalez-Casal D, González-Panizo J, Sánchez-Quintana D, Macias Y *et al.* Anatomical knowledge for the ablation of left and right atrial flutter. *Herzschrittmacherther Elektrophysiol* 2022;**33**:124–32.
36. Cabrera JA, Ho SY, Climent V, Sánchez-Quintana D. The architecture of the left lateral atrial wall: a particular anatomic region with implications for ablation of atrial fibrillation. *Eur Heart J* 2008;**29**:356–62.
37. Cabrera JA, Sánchez-Quintana D. Cardiac anatomy: what the electrophysiologist needs to know. *Heart* 2013;**99**:417–31.
38. Ho SY, Anderson RH, Sánchez-Quintana D. Atrial structure and fibres: morphologic bases of atrial conduction. *Cardiovasc Res* 2002;**54**:325–36.
39. Haïssaguerre M, Jaïs P, Shah DC, Takahashi A, Hocini M, Quiniou G *et al.* Spontaneous initiation of atrial fibrillation by ectopic beats originating in the pulmonary veins. *N Engl J Med* 1998;**339**:659–66.
40. Jaïs P, Hocini M, Macle L, Choi KJ, Deisenhofer I, Weerasooriya R *et al.* Distinctive electrophysiological properties of pulmonary veins in patients with atrial fibrillation. *Circulation* 2002;**106**:2479–85.
41. Tzeis S, Gerstenfeld EP, Kalman J, Saad EB, Sepehri Shamloo A, Andrade JG *et al.* 2024 European Heart Rhythm Association/Heart Rhythm Society/Asia Pacific Heart Rhythm Society/Latin American Heart Rhythm Society expert consensus statement on catheter and surgical ablation of atrial fibrillation. *Europace* 2024;**26**:euae043.
42. Kistler PM, Chieng D, Sugumar H, Ling LH, Segan L, Azzopardi S *et al.* Effect of catheter ablation using pulmonary vein isolation with vs without posterior left atrial wall isolation on atrial arrhythmia recurrence in patients with persistent atrial fibrillation: the CAPLA randomized clinical trial. *JAMA* 2023;**329**:127–35.
43. Caixal G, Althoff T, Garre P, Alarcón F, NuñezGarcia M, Benito EM *et al.* Proximity to the descending aorta predicts regional fibrosis in the adjacent left atrial wall: aetiopathogenic and prognostic implications. *Europace* 2021;**23**:1559–67.
44. Higuchi K, Cates J, Gardner G, Morris A, Burgon NS, Akoum N *et al.* The spatial distribution of late gadolinium enhancement of left atrial magnetic resonance imaging in patients with atrial fibrillation. *JACC Clin Electrophysiol* 2018;**4**:49–58.
45. William J, Chieng D, Curtin AG, Sugumar H, Ling LH, Segan L *et al.* Radiofrequency catheter ablation of persistent atrial fibrillation by pulmonary vein isolation with or without left atrial posterior wall isolation: long-term outcomes of the CAPLA trial. *Eur Heart J* 2025;**46**:132–43.
46. Segan L, Chieng D, Prabhu S, Hunt A, Watts T, Klys B *et al.* Posterior wall isolation improves outcomes for persistent AF with rapid posterior wall activity: CAPLA substudy. *JACC Clin Electrophysiol* 2023;**9**:2536–46.
47. Rao S, Kwasnik A, Tung R. Direct epicardial recordings in the region of the septopulmonary bundle: anatomy "behind" posterior wall activation. *JACC Clin Electrophysiol* 2020;**6**:1214–6.
48. Pambrun T, Duchateau J, Delgove A, Denis A, Constantin M, Ramirez FD *et al.* Epicardial course of the septopulmonary bundle: anatomical considerations and clinical implications for roof line completion. *Heart Rhythm* 2021;**18**:349–57.
49. Althoff TF, Garre P, Caixal G, Perea R, Prat S, Tolosana JM *et al.* Late gadolinium enhancement-MRI determines definite lesion formation most accurately at 3 months post ablation compared to later time points. *Pacing Clin Electrophysiol* 2022;**45**:72–82.
50. Benito EM, Cabanelas N, Nuñez-Garcia M, Alarcón F, Figueras I Ventura RM, Soto-Iglesias D *et al.* Preferential regional distribution of atrial fibrosis in posterior wall around left inferior pulmonary vein as identified by late gadolinium enhancement cardiac magnetic resonance in patients with atrial fibrillation. *Europace* 2018;**20**: 1959–65.
51. Müller-Edenborn B, Chen J, Allgeier J, Didenko M, Moreno-Weidmann Z, Neumann FJ *et al.* Amplified sinus-P-wave reveals localization and extent of left atrial low-voltage substrate: implications for arrhythmia freedom following pulmonary vein isolation. *Europace* 2020;**22**:240–9.
52. Althoff TF, Eichenlaub M, Padilla-Cueto D, Lehrmann H, Garre P, Schoechlin S *et al.* Predictive value of late gadolinium enhancement cardiovascular magnetic resonance in patients with persistent atrial fibrillation: dual-centre validation of a standardized method. *Eur Heart J Open* 2023;**3**:oeac085.
53. Ho SY, Anderson RH, Sánchez-Quintana D. Gross structure of the atriums: more than an anatomic curiosity? *Pacing Clin Electrophysiol* 2002;**25**:342–50.

54. Sánchez-Quintana D, Ho SY, Cabrera JA, Farré J, Anderson RH. Topographic anatomy of the inferior pyramidal space: relevance to radiofrequency catheter ablation. *J Cardiovasc Electrophysiol* 2001;**12**:210–7.
55. Blackshear JL, Odell JA. Appendage obliteration to reduce stroke in cardiac surgical patients with atrial fibrillation. *Ann Thorac Surg* 1996;**61**:755–9.
56. Whitlock RP, Belley-Cote EP, Paparella D, Healey JS, Brady K, Sharma M *et al.* Left atrial appendage occlusion during cardiac surgery to prevent stroke. *N Engl J Med* 2021;**384**: 2081–91.
57. Di Biase L, Burkhardt JD, Mohanty P, Sanchez J, Mohanty S, Horton R *et al.* Left atrial appendage: an underrecognized trigger site of atrial fibrillation. *Circulation* 2010;**122**: 109–18.
58. Anderson RH, Cook AC. The structure and components of the atrial chambers. *Europace* 2007;**9 Suppl 6**:vi3–9.
59. Restrepo AJ, Razminia M, Sánchez-Quintana D, Cabrera Rodriguez J-Á. Translational anatomy of the sinoatrial node: myoarchitecture of the sinoatrial node and its relevance for catheter ablation: anatomy and histology. *JACC Case Rep* 2024;**29**:102153.
60. O'Connor M, Barbero U, Kramer DB, Lee A, Hua A, Ismail T *et al.* Anatomic, histologic, and mechanical features of the right atrium: implications for leadless atrial pacemaker implantation. *Europace* 2023;**25**:euad235.
61. Anderson RH, Sanchez-Quintana D, Mori S, Spicer DE, Wellens HJJ, Lokhwandala Y *et al.* Miniseries 2-septal and paraseptal accessory pathways-part I: the anatomic basis for the understanding of para-Hisian accessory atrioventricular pathways. *Europace* 2022;**24**:639–49.
62. Farré J, Anderson RH, Rubio JM, García-Talavera C, Sánchez-Quintana D, Bansal R *et al.* Miniseries 2-septal and paraseptal accessory pathways-part III: mid-paraseptal accessory pathways-revisiting bypass tracts crossing the pyramidal space. *Europace* 2022;**24**: 662–75.
63. Farré J, Anderson RH, Sánchez-Quintana D, Mori S, Rubio JM, García-Talavera C *et al.* Miniseries 2-septal and paraseptal accessory pathways-part II: para-Hisian accessory pathways-so-called anteroseptal pathways revisited. *Europace* 2022;**24**:650–61.
64. Hikspoors J, Macías Y, Tretter JT, Anderson RH, Lamers WH, Mohun TJ *et al.* Miniseries 1-part I: the development of the atrioventricular conduction axis. *Europace* 2022;**24**: 432–42.
65. Badertscher P, Serban T, Isenegger C, Krisai P, Voellmin G, Osswald S *et al.* Role of 3D electro-anatomical mapping on procedural characteristics and outcomes in pulsed-field ablation for atrial fibrillation. *Europace* 2024;**26**:euae075.
66. Boersma L, Andrade JG, Betts T, Duytschaever M, Pürerfellner H, Santoro F *et al.* Progress in atrial fibrillation ablation during 25 years of Europace journal. *Europace* 2023;**25**:euad244.
67. Gunawardene MA, Harloff T, Jularic M, Dickow J, Wahedi R, Anwar O *et al.* Contemporary catheter ablation of complex atrial tachycardias after prior atrial fibrillation ablation: pulsed field vs. radiofrequency current energy ablation guided by high-density mapping. *Europace* 2024;**26**:euae072.
68. Azzolin L, Eichenlaub M, Nagel C, Nairn D, Sanchez J, Unger L *et al.* Personalized ablation vs. conventional ablation strategies to terminate atrial fibrillation and prevent recurrence. *Europace* 2022;**25**:211–22.
69. Althoff TF, Mont L. Prediction of stroke risk based on left atrial appendage morphology: from pareidolia to artificial intelligence. *Int J Cardiovasc Imaging* 2021;**37**: 2529–31.
70. Marrouche NF, Wilber D, Hindricks G, Jais P, Akoum N, Marchlinski F *et al.* Association of atrial tissue fibrosis identified by delayed enhancement MRI and atrial fibrillation catheter ablation: the DECAAF study. *JAMA* 2014;**311**:498–506.
71. El Hajjar AH, Dagher L, Younes H, Mekhael M, Noujaim C, Chouman N *et al.* History of stroke as a predictor of high left atrial fibrosis in patients with persistent atrial fibrillation-insight from the DECAAF II randomized trial. *J Interv Card Electrophysiol* 2024;**67**:2101–9.
72. King JB, Azadani PN, Suksaranjit P, Bress AP, Witt DM, Han FT *et al.* Left atrial fibrosis and risk of cerebrovascular and cardiovascular events in patients with atrial fibrillation. *J Am Coll Cardiol* 2017;**70**:1311–21.
73. Deneke T, Kutyifa V, Hindricks G, Sommer P, Zeppenfeld K, Carbucicchio C *et al.* Pre- and post-procedural cardiac imaging (computed tomography and magnetic resonance imaging) in electrophysiology: a clinical consensus statement of the European Heart Rhythm Association and European Association of Cardiovascular Imaging of the European Society of Cardiology. *Europace* 2024;**26**:euae108.